Electronic Supplementary Information (ESI)

Experimental Study of Speciation and Mechanistic Implications when Using Chelating Ligands in Aryl–Alkynyl Stille Coupling

Ana M. Gallego, Marconi N. Peñas-Defrutos, Guillermo Marcos-Ayuso, Jose M. Martín-Alvarez, Jesús M. Martínez-Ilarduya and Pablo Espinet*

IU CINQUIMA/Química Inorgánica, Facultad de Ciencias, Universidad de Valladolid, E–47071 Valladolid, Spain

E–mail: espinet@qi.uva.es

1. General information

All reactions were carried out under nitrogen atmosphere using Schlenk-tube techniques. Dichloromethane (DCM), diethylether (Et_2O) and hexane were obtained oxygen- and water-free from an SPS PS–MD–5 solvent purification apparatus. Toluene and tetrahydrofuran (THF) were dried by the usual procedures and distilled under argon prior to being used.[1]

The technical measurements were carried out with equipment of the LTI services or the IU CINQUIMA (both of the University of Valladolid) unless otherwise stated.

^1H, ^{19}F and $^{31}P\{^1H\}$ NMR spectra were run on a Bruker AV–400 and/or a Varian 500/54 Premium Shielded instrument. Chemical shifts (in δ units, parts per million) were referenced to the residual solvent peaks (^1H),[2] external 85% H_3PO_4 ($^{31}P\{^1H\}$) or $CFCl_3$ (^{19}F). Coupling constants (*J*) are given in hertz (Hz). The following abbreviations are used to describe peak patterns when appropriate: s (singlet), d (doublet), t (triplet), q (quartet), m (multiplet), br (broad). A capillary of acetone-d_6 was used for the lock if the solvents of the samples were nondeuterated.

Infrared spectra were recorded with Perkin–Elmer Frontier (4000-200 cm^{-1}) equipped with an ATR accessory (*Attenuated Total Reflection*) for the direct registration of solid samples.

The elemental analyses were performed by the Elemental Analysis Unit of the University of Vigo on a Carlo Erba 1108 CHN analyzer.

Conductivity measures were carried out by a Mettler Toledo MC226 conductivity meter.

$[Pd(Rf)_2(dppe)]$ was prepared using the same procedure described for *cis*-$[Pd(Rf)_2(PPh_3)_2]$.[3] PhC≡CRf was synthesized as previously reported.[4] PhC≡C$SnBu_3$ was purchased from Sigma Aldrich.

2. Synthesis of [Pd(Rf)Cl(P-L)] (2)

In a general procedure, to a solution of $(\mu\text{–Cl})_2[Pd_2(Rf)_2(tht)_2]$[3] (**1**) (223.6 mg, 0.26 mmol) in CH_2Cl_2 (25 mL) phosphine (P-P or P-L) (0.52 mmol) was added and the mixture was stirred for 45 minutes. The solvent was evaporated to dryness and diethyl ether (10 mL) was added. The solid obtained was filtered off, washed with diethyl ether and dried under vacuum to afford the pure product.

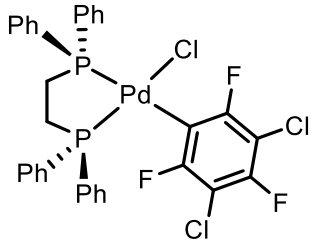

[Pd(Rf)Cl(dppe)] (2a)

Using 1,2-bis(diphenylphosphino)ethane (dppe) (207.2 mg, 0.52 mmol) and following the general procedure, product **2a** was isolated as a white solid. **Yield**: 361.8 mg (94%).

Anal. Calcd for $C_{32}H_{24}Cl_3F_3P_2Pd$: C, 51.92; H, 3.27. Found: C, 51.87; H, 3.46. **^{1}H NMR** (499.72 MHz, $CDCl_3$, 298 K) δ (ppm): 7.94 (m, 4H, Ph), 7.55-7.45 (12H, Ph), 7.36 (m, 4H, Ph), 2.53 (m, 2H, CH_2), 2.19 (m, 2H, CH_2). **^{19}F NMR** (470.16 MHz, $CDCl_3$, 298 K) δ (ppm): –90.94 (dd, 2F, $^4J_{F–P(trans)}$ = 14.0 Hz, $^4J_{F–P(cis)}$ = 5.8 Hz, F^o), –119.22 (s, 1F, F^p). **^{31}P{^{1}H} NMR** (202.31 MHz, $CDCl_3$, 298 K) δ (ppm): 58.4 (dt, $^2J_{P–P}$ = 16.5 Hz, $^4J_{P–F}$ = 5.8 Hz, P_{cis}), 43.4 (dt, $^2J_{P–P}$ = 16.5 Hz, $^4J_{P–F}$ = 14.0 Hz, P_{trans}). $\mathbf{\Lambda_M}$ (5×10^{-4} M, 298 K, THF) = 0.1 S cm^2 mol^{-1}.

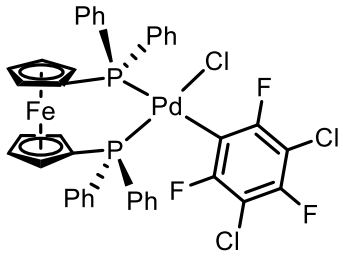

[Pd(Rf)Cl(dppf)] (2b)

Using 1,2-bis(diphenylphosphino)ferrocene (dppf) (288.3 mg, 0.52 mmol) and following the general procedure, product **2b-dim** precipitated as a yellow orange solid in CH_2Cl_2. **Yield**: 23.3 mg (5%). Once this solid was separated the workup led to the isolation of **2b** as an orange solid. **Yield**: 386.8 mg (83%). Crystals of **2b** valid for X-Ray diffraction analysis were obtained by slow diffusion of *n*-hexane in a solution of the compound in CH_2Cl_2. Crystals of **2b-dim**·$2CH_2Cl_2$ valid for X-Ray diffraction analysis were obtained mixing two solutions of the reactants in CH_2Cl_2 and leaving the mixture without stirring.

2b: Anal. Calcd for $C_{40}H_{28}Cl_3F_3FeP_2Pd$: C, 53.61; H, 3.15. Found: C, 53.58; H, 3.22. **^{1}H NMR** (499.72 MHz, $CDCl_3$, 298 K) δ (ppm): 8.06 (m, 4H, Ph), 7.55-7.35 (10H, Ph), 7.33 (m, 2H, Ph), 7.13 (m, 4H, Ph), 4.95 (m, 2H, C_5H_4), 4.59 (m, 2H, C_5H_4), 4.18 (m, 2H, C_5H_4), 3.39 (m, 2H, C_5H_4). **^{19}F NMR** (470.16 MHz, $CDCl_3$, 298 K) δ (ppm): –93.26 (dd, 2F, $^4J_{F–P(trans)}$ = 13.4 Hz, $^4J_{F–P(cis)}$ = 8.8 Hz, F^o), –120.11 (s, 1F, F^p). **^{31}P{^{1}H} NMR** (202.31 MHz,

$CDCl_3$, 298 K) δ (ppm): 33.2 (dt, $^2J_{P–P}$ = 14.8 Hz, $^4J_{P–F}$ = 8.8 Hz, P_{cis}), 15.9 (dt, $^2J_{P–P}$ = 14.8 Hz, $^4J_{P–F}$ = 13.4 Hz, P_{trans}).

2b-dim: **Anal. Calcd** for $C_{80}H_{56}Cl_6F_6Fe_2P_4Pd_2$: C, 53.61; H, 3.15. Found: C, 53.41; H, 3.23. **^{1}H NMR** (400.14 MHz, THF-d_8, 298 K) δ 8.59 (m, 8H, Ph), 7.70 (m, 12H, Ph), 6.83 (m, 4H, Ph), 6.72 (m, 8H, Ph), 6.38 (m, 8H, Ph), 5.95 (m, 4H, C_5H_4), 4.40 (m, 4H, C_5H_4), 4.36 (m, 4H, C_5H_4), 4.27 (m, 4H, C_5H_4). **^{19}F NMR** (376.50 MHz, THF-d_8, 298 K) δ –90.52 (t, 2F, $^4J_{F-P}$ = 7.7 Hz, F^o), –90.69 (t, 2F, $^4J_{F-P}$ = 6.6 Hz, F^o), –122.01 (t, 2F, $^6J_{F-P}$ = 2.5 Hz, F^p). **^{31}P{^{1}H} NMR** (161.98 MHz, THF-d_8, 298 K) δ 19.8 (m, 4P).

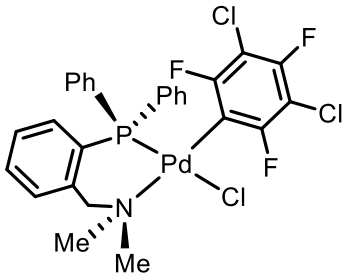

[Pd(Rf)Cl{PPh_2(bzN)}] (2c)

Using the aminophosphine PPh_2(bzN)[5] (166.1 mg, 0.52 mmol) and following the general procedure, product **2c** is isolated as a yellow solid. **Yield**: 292.3 mg (85%).

Anal. Calcd for $C_{27}H_{22}Cl_3F_3NPPd$: C, 49.05; H, 3.35; N, 2.12. Found: C, 48.90; H, 3.37; N, 2.32. **^{1}H NMR** (499.72 MHz, $CDCl_3$, 298 K) δ (ppm): 7.60-7.27 (m, 14H, Ph + C_6H_4), 3.30 (br, 2H, CH_2), 2.98 (br, 6H, NMe_2). **^{19}F NMR** (470.16 MHz, $CDCl_3$, 298 K) δ (ppm): –82.53 (vbr, 1F, F^o), –88.38 (vbr, 1F, F^o), –119.03 (s, 1F, F^p). **^{31}P{^{1}H} NMR** (202.31 MHz, $CDCl_3$, 298 K) δ (ppm): 20.5 (td, $^4J_{P–F}$ = 9.1 Hz, $^6J_{P–F}$ = 4.0 Hz, 1P).

3. Synthesis of [Pd(Rf)I(P-L)] (**3**)

In a general procedure, [Pd(Rf)Cl(P-L)] (**2**) (0.16 mmol) and KI (33.2 mg, 0.20 mmol) were mixed in acetone/CH_2Cl_2 (15/15 mL), stirred for 1 hour and then evaporated to dryness. The residue was extracted in CH_2Cl_2 (10 mL) and evaporated again. The solid obtained was washed with diethyl ether/*n*-hexane and vacuum-dried.

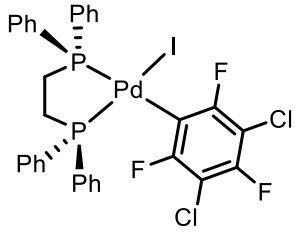

[Pd(Rf)I(dppe)] (3a)

Using the [Pd(Rf)Cl(dppe)] (**2a**) (118.4 mg, 0.16 mmol) and following the general procedure, product **3a** is isolated as a yellow solid. **Yield**: 111.8 mg (84%).

Anal. Calcd for $C_{32}H_{24}Cl_2F_3IP_2Pd$: C, 46.21; H, 2.91. Found: C, 46.09; H, 3.02. **^{1}H NMR** (499.72 MHz, $CDCl_3$, 298 K) δ (ppm): 7.85 (m, 4H, Ph), 7.57-7.45 (m, 12H, Ph), 7.38 (m, 4H, Ph), 2.43-2.20 (m, 4H, CH_2). **^{19}F NMR** (470.16 MHz, $CDCl_3$, 298 K) δ (ppm): –89.06 (dd, 2F, $^4J_{F–P(trans)}$ = 13.3 Hz, $^4J_{F–P(cis)}$ = 5.0 Hz, F^o), –119.54 (s, 1F, F^p). **^{31}P{^{1}H} NMR** (202.31 MHz, $CDCl_3$, 298 K) δ (ppm): 55.2 (dt, $^2J_{P–P}$ = 15.5 Hz, $^4J_{P–F}$ = 5.0 Hz, P_{cis}), 45.6 (dt, $^2J_{P–P}$ = 15.5 Hz, $^4J_{P–F}$ = 13.3 Hz, P_{trans}). $\mathbf{\Lambda_M}$ (5×10^{-4} M, 298 K, HMPA) = 15 S cm^2 mol^{-1}; $\mathbf{\Lambda_M}$ (5×10^{-4} M, 298 K, NMP) = 1 S cm^2 mol^{-1}.

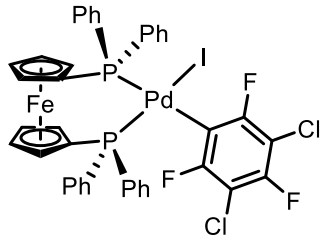

[Pd(Rf)I(dppf)] (3b)

Using the [Pd(Rf)Cl(dppf)] (**2b**) (143.4 mg, 0.16 mmol) and following the general procedure, product **3b** is isolated as an orange solid. **Yield**: 124.8 mg (79%).

Anal. Calcd for $C_{40}H_{28}Cl_2F_3FeIP_2Pd$: C, 48.64; H, 2.86 Found: C, 48.33; H, 3.10. **^{1}H NMR** (499.72 MHz, $CDCl_3$, 298 K) δ (ppm): 8.09 (m, 4H, Ph), 7.56-7.36 (10H, Ph), 7.36 (m, 2H, Ph), 7.13 (m, 4H, Ph), 4.95 (m, 2H, C_5H_4), 4.59 (m, 2H, C_5H_4), 4.18 (m, 2H, C_5H_4), 3.39 (m, 2H, C_5H_4). **^{19}F NMR** (470.16 MHz, $CDCl_3$, 298 K) δ (ppm): –93.60 (dd, 2F, $^4J_{F–P(trans)}$ = 13.6 Hz, $^4J_{F–P(cis)}$ = 8.8 Hz, F^o), –120.44 (s, 1F, F^p). **^{31}P{^{1}H} NMR** (202.31 MHz, $CDCl_3$, 298 K) δ (ppm): 33.7 (dt, $^2J_{P–P}$ = 15.0 Hz, $^4J_{P–F}$ = 8.8 Hz, P_{cis}), 16.5 (dt, $^2J_{P–P}$ = 15.0 Hz, $^4J_{P–F}$ = 13.6 Hz, P_{trans}). $\mathbf{\Lambda_M}$ (5×10^{-4} M, 298 K, HMPA) = 14 S cm^2 mol^{-1}; $\mathbf{\Lambda_M}$ (5×10^{-4} M, 298 K, NMP) = 2 S cm^2 mol^{-1}.

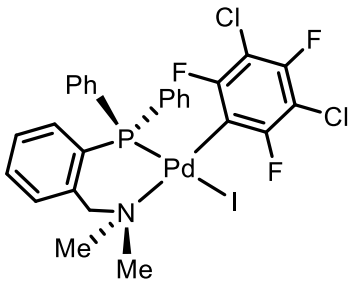

[Pd(Rf)I{PPh$_2$(bzN)}] (3c)

Using the [Pd(Rf)Cl{PPh$_2$(bzN)}] (**2c**) (105.8 mg, 0.16 mmol) and following the general procedure, product **3c** is isolated as a pink solid. **Yield**: 91.5 mg (76%). Crystals of **3c**·THF valid for X-Ray diffraction analysis were obtained by slow diffusion of *n*-hexane in a solution of **3c** in THF.

Anal. Calcd for $C_{27}H_{22}Cl_2F_3INPPd$: C, 43.09; H, 2.95; N, 1.86. Found: C, 42.95; H, 3.29; N, 1.90. **^{1}H NMR** (499.72 MHz, $CDCl_3$, 298 K) δ (ppm): 7.59–7.27 (m, 14H, Ph + C_6H_4), 3.30 (br, 2H, CH_2), 2.99 (br, 6H, NMe_2). **^{19}F NMR** (470.16 MHz, $CDCl_3$, 298 K) δ (ppm): –83.50 (vbr, 1F, F^o), –89.50 (vbr, 1F, F^o), –120.40 (s, 1F, F^p). **^{31}P{^{1}H} NMR** (202.31 MHz, $CDCl_3$, 298 K) δ (ppm): 20.5 (td, $^4J_{P–F}$ = 8.0 Hz, $^6J_{P–F}$ = 4.0 Hz, 1P). $\mathbf{\Lambda_M}$ (5×10^{-4} M, 298 K, HMPA) = 15 S cm^2 mol^{-1}; $\mathbf{\Lambda_M}$ (5×10^{-4} M, 298 K, NMP) = 2 S cm^2 mol^{-1}.

4. Synthesis of [Pd(Rf)(OTf)(P-L)] (4)

In a general procedure, to a solution of AgOTf (51.4 mg, 0.20 mmol) in acetone/CH_2Cl_2 (10/10 mL) shielded from the light, [Pd(Rf)Cl(P-L)] (**2**) (0.20 mmol) was added and the mixture was stirred for 45 min. The AgCl formed was carefully filtered out, and the solution was evaporated to dryness. The residue was treated with diethyl ether/*n*-pentane (3/6 mL) and the solid obtained was filtered off, dried under vacuum and heated in an oven at 50 °C up to constant weight (about two days).

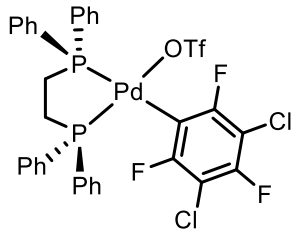

[Pd(Rf)(OTf)(dppe)] (4a)

Using the [Pd(Rf)Cl(dppe)] (**2a**) (148.1 mg, 0.20 mmol) and following the general procedure, product **4a** is isolated as a white solid. **Yield**: 143.5 mg (84%).

Anal. Calcd for $C_{33}H_{24}Cl_2F_6O_3P_2PdS$: C, 46.42; H, 2.83. Found: C, 46.28; H, 2.71. **IR** (Nujol-polyethylene, cm^{-1}): 1230 (vs, st S–O), 1210 (vs, st S–O), 1191 (vs, st S-O), 770 (s, st Pd–R). **^{1}H NMR** (499.72 MHz, $CDCl_3$, 298 K) δ (ppm): 7.81 (m, 4H, Ph), 7.61-7.51 (m, 12H, Ph), 7.41 (m, 4H, Ph), 2.58 (m, 2H, CH_2), 2.17 (m, 2H, CH_2). **^{19}F NMR** (470.16 MHz, $CDCl_3$, 298 K) δ (ppm): –77.71 (s, 3F, CF_3), –89.95 (dd, 2F, $^4J_{F–P(trans)}$ = 13.1 Hz, $^4J_{F–P(cis)}$ = 7.2 Hz, F^o), –116.87 (s, 1F, F^p)**. ^{31}P{^{1}H} NMR** (202.31 MHz, $CDCl_3$, 298 K) δ (ppm): 60.9 (dt, $^2J_{P–P}$ = 15.4 Hz, $^4J_{P–F}$ = 7.2 Hz, P_{cis}), 45.3 (dt, $^2J_{P–P}$ = 15.4 Hz, $^4J_{P–F}$ = 13.1 Hz, P_{trans}). Λ_M (5×10^{-4} M, 298 K, THF) = 4 S cm^2 mol^{-1}.

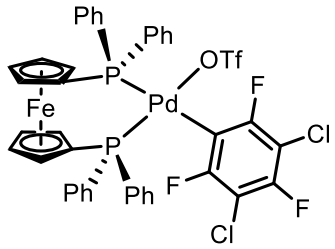

[Pd(Rf)(OTf)(dppf)] (4b)

Using the [Pd(Rf)Cl(dppf)] (**2b**) (179.2 mg, 0.20 mmol) and following the general procedure, product **4b** is isolated as an orange solid. **Yield**: 169.7 mg (84%).

Anal. Calcd for $C_{41}H_{28}Cl_2F_6FeO_3P_2PdS$: C, 48.77; H, 2.79 Found: C, 48.78; H, 2.47. **IR** (Nujol-polyethylene, cm^{-1}): 1231 (vs, st S–O), 1204 (vs, st S–O), 1173 (vs, st S–O), 696 (vs, st Pd–R**). ^{1}H NMR** (499.72 MHz, $CDCl_3$, 298 K) δ (ppm): 7.88 (m, 4H, Ph), 7.62-7.36 (m, 12H, Ph), 7.14 (m, 4H, Ph), 5.30 (m, 2H, C_5H_4), 5.06 (m, 2H, C_5H_4), 4.67(m, 2H, C_5H_4), 4.26 (m, 2H, C_5H_4). **^{19}F NMR** (470.16 MHz, $CDCl_3$, 298 K) δ (ppm): –78.43 (s, 3F, CF_3), –93.91 (s, 2F, F^o), –116.88 (s, 1F, F^p)**. ^{31}P{^{1}H} NMR** (202.31 MHz, $CDCl_3$, 298 K) δ (ppm): 38.7 (m, P_{cis}), 17.2 (m, P_{trans}). Λ_M (5×10^{-4} M, 298 K, THF) = 4 S cm^2 mol^{-1}.

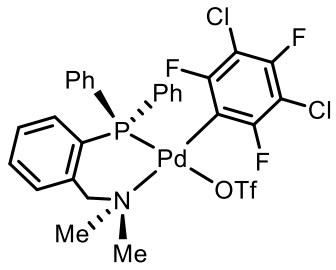

[Pd(Rf)(OTf){PPh_2(bzN)}] (4c)

Using the [Pd(Rf)Cl{PPh_2(bzN)}] (**2c**) (132.2 mg, 0.20 mmol) and following the general procedure, product **4c** is isolated as a yellow solid. **Yield**: 125.5 mg (81%). Crystals of [Pd(Rf)(OH_2){PPh_2(bzN)}](TfO)·CH_2Cl_2 (**5c**·CH_2Cl_2) valid for X-Ray diffraction analysis were obtained by slow diffusion of *n*-hexane in a solution of **4c** in wet CH_2Cl_2.

Anal. Calcd for $C_{28}H_{22}Cl_2F_6NO_3PPdS$: C, 43.40; H, 2.86; N, 1.81. Found: C, 43.15; H, 2.79; N, 1.86. **IR** (Nujol-polyethylene, cm^{-1}): 1234 (vs, st S–O), 1211 (vs, st S–O), 1181(s, st S–O), 695 (s, st Pd–R). **^{1}H NMR** (499.72 MHz, $CDCl_3$, 298 K) δ (ppm): 7.65–7.28 (m, 14H, Ph + C_6H_4), 3.24 (br, 2H, CH_2), 2.73 (br, 6H, NMe_2). **^{19}F NMR** (470.16 MHz, $CDCl_3$, 298 K) δ (ppm): –77.86 (s, 3F, CF_3), –91.43 (d, 2F, $^4J_{F–P}$ = 10.7 Hz, F^o), –117.38 (s, 1F, F^p). **^{31}P{^{1}H}** NMR (202.31 MHz, $CDCl_3$, 298 K) δ (ppm): 30.5 (t, $^4J_{P–F}$ = 10.7 Hz). Λ_M (5 × 10^{-4} M, 298 K, THF) = 4 S cm^2 mol^{-1}.

5. Characterization of [Pd(Rf)(C≡CPh)(dppe)](11a)

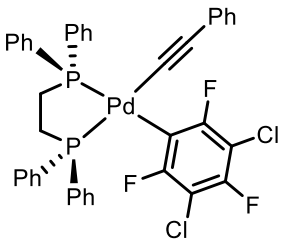

[Pd(Rf)(C≡CPh)(dppe)] (11a)

To a solution of [Pd(Rf)(OTf)(dppe)] (**4a**) (50 mg, 0.059 mmol) in dry and deoxygenated THF (3 mL) in a 10 mL Schlenk tube, $PhC{\equiv}CSnBu_3$ (205 μL, 0.586 mmol) was added and the mixture was stirred for 5 min. After that, *n*-hexane (5 mL) is placed on top of the yellow solution forming an interphase and the Schlenk tube was stored at –28 ºC. After two days, crystals of **11a**·0.75THF valid for X-Ray diffraction were obtained.

^{19}F NMR (470.16 MHz, THF/cap. acetone-d_6, 298 K) δ (ppm): –90.61 (dd, 2F, $^4J_{F\text{-}P(trans)}$ = 12.5 Hz, $^4J_{F\text{-}P(cis)}$ = 3.1 Hz, F^o), –123.69 (s, 1F, F^p). **^{31}P{^{1}H} NMR** (202.31 MHz, THF/cap. acetone-d_6, 298 K) δ (ppm): 55.2 (d, $^2J_{P\text{-}P}$ = 20.6 Hz, P_{cis}), 50.4 (dt, $^2J_{P\text{-}P}$ = 20.6 Hz, $^4J_{P\text{-}F}$ = 12.5 Hz, P_{trans}).

6. X-Ray diffraction details

Refinement of the X-Ray structures gives the residuals shown in Tables S1 and S2. A crystal was attached to a glass fiber or a micromount and transferred to an Agilent Supernova diffractometer with an Atlas CCD area detector. Data collection was performed with Mo-Kα radiation (λ = 0.71073 Å). Data integration, scaling and empirical absorption correction was carried out using the CrysAlisPro program package.[6] The crystal was kept at 294 K or 210 K during data collection. Using Olex2,[7] the structure was solved with the ShelxT,[8] and refined with ShelxL program.[9] The non-hydrogen atoms were refined anisotropically and hydrogen atoms were placed at idealized positions and refined using the riding model. Refinement proceeded smoothly to give the residuals shown in Tables ESI1 and ESI2. CCDC 1999841-1999845 and 2012676 contain the supporting crystallographic data for this paper. These data can be obtained free of charge at www.ccdc.cam.ac.uk/conts/retrieving.html [or from the Cambridge Crystallographic Data Centre, 12, Union Road, Cambridge CB2 1EZ, UK; fax: (internat.) +44-1223/336-033; E-mail: deposit@ccdc.cam.ac.uk].

Crystal structures of [Pd(Rf)Cl(dppf)] (**2b**) and [Pd(Rf)I{PPh_2(bzN)}] (**3c**) are shown in Figures ESI1 and ESI2 respectively.

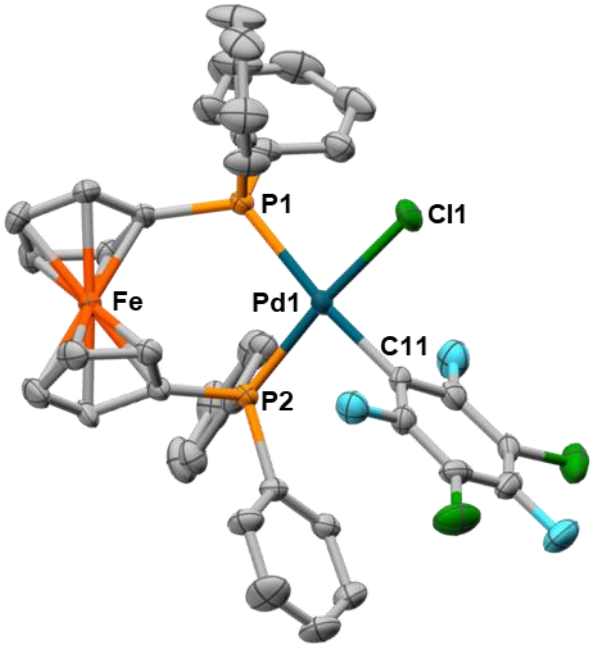

Figure ESI 1. Molecular structure of **2b**. Hydrogen atoms are omitted for clarity. Selected bond lengths (Å) and angles (°): Pd(1)–Cl(1) = 2.3480(9), Pd(1)–P(1) = 2.3497(9), Pd(1)–P(2) = 2.2699(9), Pd(1)–C(11) = 2.029(3), P(1)–Pd(1)–P(2) = 100.55(3).

Note that in the crystalline structure of the monomer **2b**, the Cp groups of dppf are alternated, and the Fe atom is 0.91 Å above the Pd coordination plane. However, in the dimeric **2b-dim** (Figure 2 of the main article) the ferrocenyl groups of the bridging dppf ligands are arranged as eclipsed Cp groups and the coordination planes of the two Pd atoms lie parallel to each other.

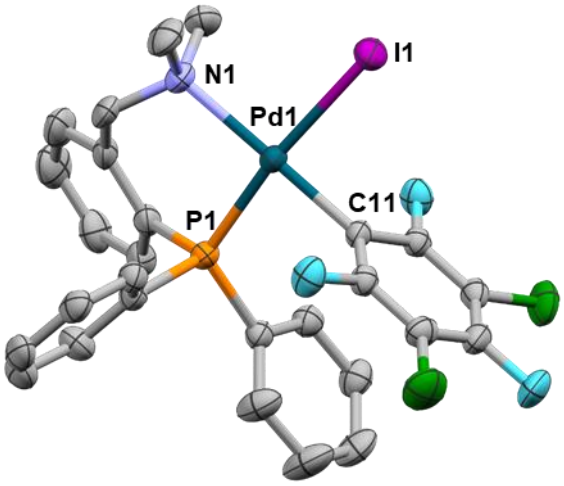

Figure ESI 2. Molecular structure of **3c**. Hydrogen atoms and crystallisation solvent molecules are omitted for clarity. Selected bond lengths (A) and bond angles (°): Pd(1)–P(1) = 2.2547(14); Pd(1)–C(11) = 2.015(5); Pd(1)–N(1) = 2.192(4); Pd(1)–I(1) = 2.6567(6). N(1)–Pd(1)–P(1) = 91.68(13).

The water hydrogen atoms of [Pd(Rf)(OH_2){PPh_2(bzN)}](TfO) (**5c**) are involved in hydrogen bonding to the triflate anions, giving rise to dimers in the crystal (Figure ESI3).

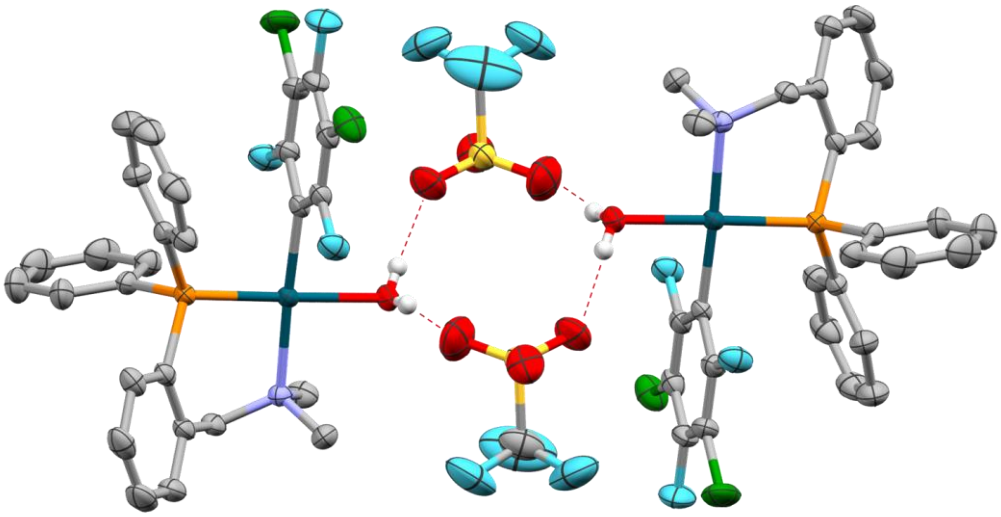

Figure ESI 3. View of the packing of **5c.**

Table ESI 1. Crystal data and structure refinements for complexes **2b**, **2b-dim**·$2CH_2Cl_2$ and **3c**·THF.

	2b	**2b-dim**·$2CH_2Cl_2$	**3c**·THF
Empirical formula	$C_{40}H_{28}Cl_3F_3FeP_2Pd$	$C_{82}H_{60}Cl_{10}F_6Fe_2P_4Pd_2$	$C_{31}H_{30}Cl_2F_3INOPPd$
Formula weight	896.16	1962.18	824.73
Temperature/K	294	294	294
Crystal system	monoclinic	triclinic	triclinic
Space group	$P2_1/n$	P-1	P-1
a/Å	13.2042(4)	12.1035(8)	10.9025(7)
b/Å	19.5582(5)	13.6408(11)	13.2759(7)
c/Å	14.3252(4)	14.2807(9)	13.4660(6)
α/°	90	102.276(6)	118.557(5)
β/°	102.932(3)	104.322(6)	100.420(5)
γ/°	90	114.833(7)	96.292(5)
Volume/$Å^3$	3605.66(18)	1934.3(3)	1639.79(17)
Z	4	1	2
$\rho_{calc}g/cm^3$	1.651	1.684	1.67
μ/mm^{-1}	1.258	1.314	1.761
F(000)	1792	980	812
Crystal size/mm^3	0.209 × 0.183 × 0.089	0.162 × 0.089 × 0.043	0.194 × 0.113 × 0.075
Radiation	MoKα (λ = 0.71073)	MoKα (λ = 0.71073)	MoKα (λ = 0.71073)
2θ range for data collection/°	6.666 to 59.098	6.612 to 59.246	6.674 to 59.514
Index ranges	$-12 \le h \le 18$, $-26 \le k \le 26$, $-19 \le l \le 18$	$-16 \le h \le 15$, $-13 \le k \le 18$, $-19 \le l \le 19$	$-14 \le h \le 13$, $-18 \le k \le 18$, $-17 \le l \le 18$
Reflections collected	19703	13550	14069
Independent reflections	8618 [R_{int} = 0.0389, R_{sigma} = 0.0623]	8808 [R_{int} = 0.0655, R_{sigma} = 0.1868]	7736 [R_{int} = 0.0298, R_{sigma} = 0.0590]
Data/restraints/parameters	8618/0/451	8808/0/478	7736/0/347
Goodness-of-fit on F^2	1.018	1.074	1.041
Final R indexes [I>=2σ (I)]	R_1 = 0.0452, wR_2 = 0.0879	R_1 = 0.0882, wR_2 = 0.1101	R_1 = 0.0490, wR_2 = 0.1113
Final R indexes [all data]	R_1 = 0.0819, wR_2 = 0.1054	R_1 = 0.1923, wR_2 = 0.1526	R_1 = 0.0860, wR_2 = 0.1399
Largest diff. peak/hole / $eÅ^{-3}$	0.60/-0.70	0.80/-1.04	0.81/-0.93

Table ESI 2. Crystal data and structure refinements for complexes **5c**·CH_2Cl_2, **11a**·0.75THF and **14a.**

	5c·CH_2Cl_2	**11a**·0.75THF	**14a**
Empirical formula	$C_{29}H_{26}Cl_4F_6NO_4PPdS$	$C_{43}H_{35}Cl_2F_3O_{0.75}P_2Pd$	$C_{46}H_{56}P_2PdSn$
Formula weight	877.74	859.95	895.93
Temperature/K	294	210.1(3)	294
Crystal system	monoclinic	monoclinic	monoclinic
Space group	C2/c	$P2_1/c$	P21/n
a/Å	29.6077(6)	43.4249(10)	10.3519(4)
b/Å	12.1976(3)	9.8871(2)	9.1916(4)
c/Å	19.6966(4)	18.8438(5)	46.0458(19)
α/°	90	90	90
β/°	97.086(2)	97.664(2)	93.940(3)
γ/°	90	90	90
Volume/$Å^3$	7059.0(3)	8018.2(3)	4370.9(3)
Z	8	8	4
$\rho_{calc}g/cm^3$	1.652	1.425	1.361
μ/mm^{-1}	1	0.721	1.085
F(000)	3504	3488	1832.0
Crystal size/mm^3	0.341 × 0.172 × 0.125	0.362 × 0.152 × 0.093	0.221 × 0.139 × 0.112
Radiation	MoKα (λ = 0.71073)	MoKα (λ = 0.71073)	MoKα (λ = 0.71073)
2θ range for data collection/°	6.998 to 58.924	6.686 to 59.2	6.774 to 59.388
Index ranges	-37 ≤ h ≤ 27, -16 ≤ k ≤ 15, -27 ≤ l ≤ 23	-60 ≤ h ≤ 57, -13 ≤ k ≤ 11, -25 ≤ l ≤ 19	13 ≤ h ≤ 14, -12 ≤ k ≤ 12, -57 ≤ l ≤ 43
Reflections collected	14916	34635	30091
Independent reflections	8267 [R_{int} = 0.0211, R_{sigma} = 0.0379]	18695 [R_{int} = 0.0391, R_{sigma} = 0.0817]	10725 [R_{int} = 0.0712, R_{sigma} = 0.1011]
Data/restraints/parameters	8267/0/434	18695/1/955	10725/5/424
Goodness-of-fit on F^2	1.035	1.096	1.105
Final R indexes [I>=2σ (I)]	R_1 = 0.0415, wR_2 = 0.0906	R_1 = 0.0754, wR_2 = 0.1449	R_1 = 0.0973, wR_2 = 0.1700
Final R indexes [all data]	R_1 = 0.0624, wR_2 = 0.1035	R_1 = 0.1258, wR_2 = 0.1687	R_1 = 0.1646, wR_2 = 0.1945
Largest diff. peak/hole / $eÅ^{-3}$	0.71/-0.49	0.91/-0.48	0.82/-1.12

7. Thermodynamic parameters for the neutral ⇌ ionic equilibria of [Pd(Rf)(OTf)(P-L)] (4) in THF solutions

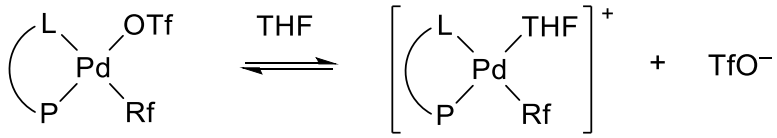

4 **6**

NMR tubes (5 mm) were charged with the corresponding triflate complexes [Pd(Rf)(OTf)(P-L)] (P-L = dppf, **4b**; PPh_2(bzN), **4c**) (0.006 mmol) which were dissolved under N_2 in dry THF and taken to a volume of 600 µL (concentration: 10^{-2} mol L^{-1}). An acetone-d_6 capillary (for NMR lock) was added, and the tubes were placed into a thermostated probe at 183 K (the temperature was checked by a methanol standard method)[10] in a Bruker Avance 400 Ultrashield apparatus. After 10 min, ^{19}F NMR spectra were carefully acquired using relaxation times long enough for meaningful integration of the signals observed (**4b**/**6b**; **4c**/**6c**). This experiment was repeated at different temperatures (Figures ESI4 and ESI6) and the numerical analysis of the data (integrals) led to the graphics collected in Figures ESI5 and ESI7. Using the values obtained by the linear fitting and following formulas, ΔH^o, ΔS^o and $K_{323\,K}$ can be calculated and the values are reported in Table S3.

$$\Delta G^o = \Delta H^o - T\Delta S^o \qquad \Delta G^o = -RT\ln K \qquad -\ln K = \frac{\Delta H}{R}\frac{1}{T} - \frac{\Delta S}{R}$$

Table ESI 3. Thermodynamic parameters for the neutral ⇌ ionic equilibria of [Pd(Rf)(OTf)(P-L)] (P-L = dppf, **4b**; PPh_2(bzN), **4c**) in THF solutions ([Pd] = 10^{-2} M).

Equilibrium	**ΔH^o** (kJ mol^{-1})	**ΔS^o**(J K^{-1} mol^{-1})	**$K_{323\,K}$**
4b ⇌ 6b	–18.4 ± 0.9	–77 ± 4	0.085
4c ⇌ 6c	–15.5 ± 0.6	–74 ± 3	0.043

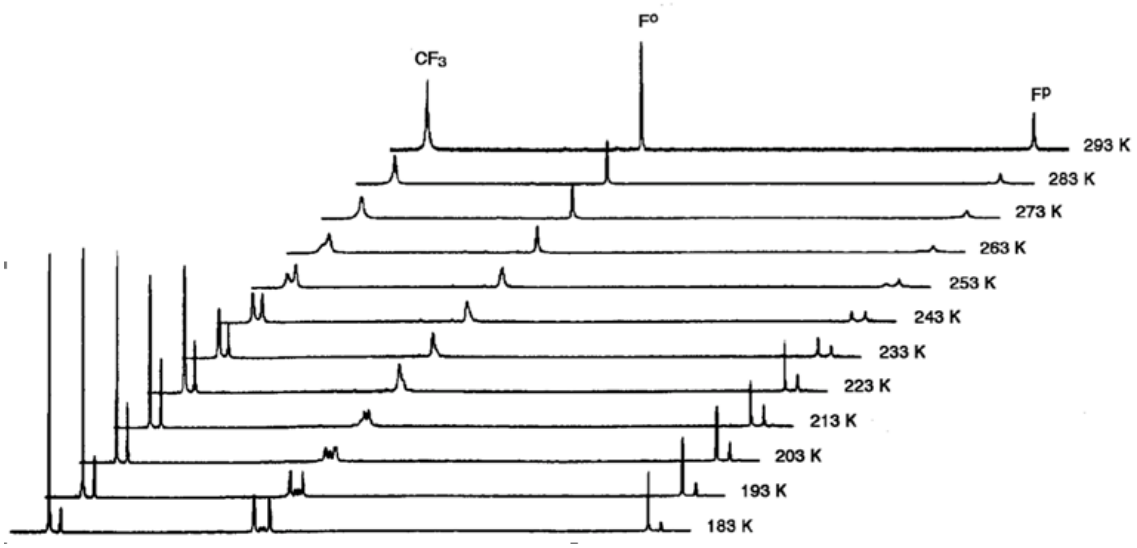

Figure ESI 4. Full ^{19}F NMR spectra of **4b** in THF at variable temperature.

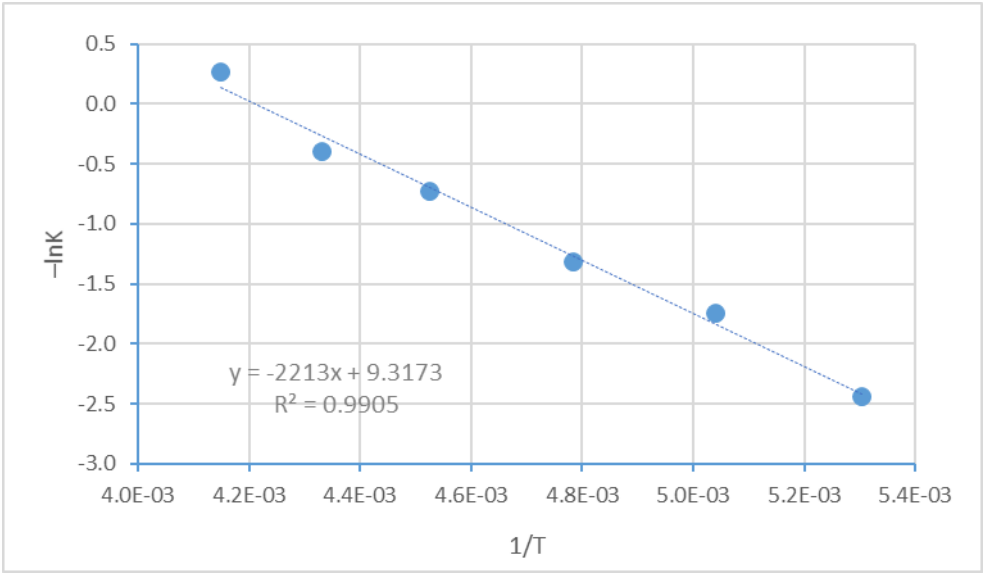

Figure ESI 5. Graphic representation and linear fitting of –lnK vs. 1/T, being K_{eq} = [**6b**]/[**4b**][11]. Temperature range: 193-243 K.

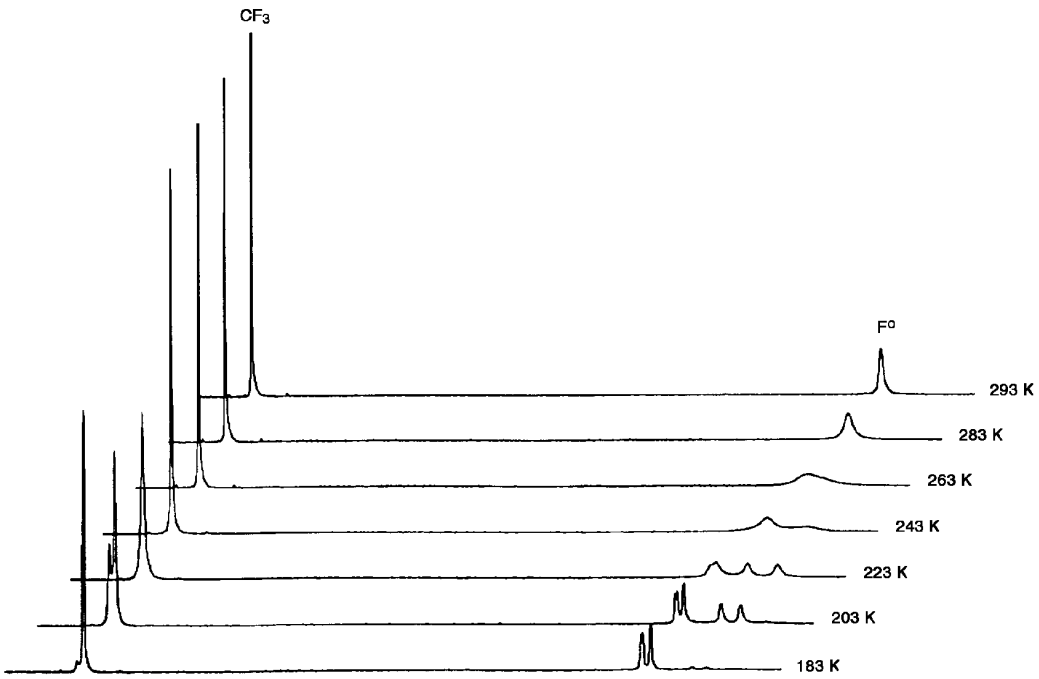

Figure ESI 6. Full ^{19}F NMR spectra of **4c** in THF at variable temperature.

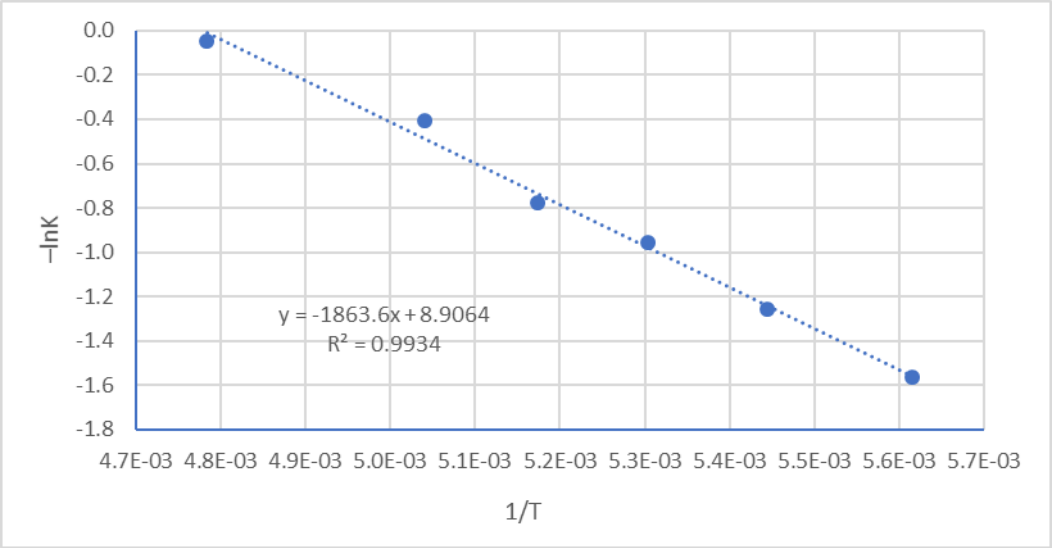

Figure ESI 7. Graphic representation and linear fit of –lnK vs. 1/T, being K_{eq} = [**6c**]/[**4c**]. Temperature range: 183-213 K.

8. Behaviour of [Pd(Rf)X(P-L)] in NMP and HMPA solutions

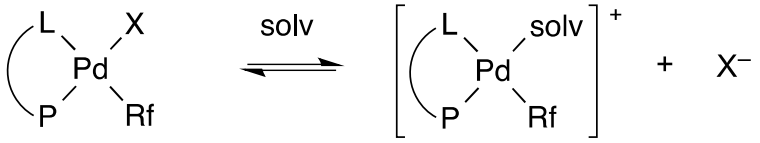

NMR tubes were charged with two samples of [Pd(Rf)X(P-L)] (0.006 mmol) which were dissolved under N_2 in dry NMP and HMPA and taken to a volume of 600 µL (concentration: 10^{-2} mol L^{-1}). An acetone-d_6 capillary (for NMR lock) was introduced, and the tubes were placed into a thermostated probe at 323 K (the temperature was checked by an ethylene glycol standard method)[10] in a Bruker Avance 400 Ultrashield apparatus. After 10 min, ^{19}F NMR spectra were carefully acquired using relaxation times long enough for meaningful integration of the signals observed. After that, these solutions were transferred to two different tubes containing $AgBF_4$ (0.006 mmol), the mixtures were shaken for 2 min and the ^{19}F NMR spectra were acquired again. Comparison of the NMR spectra in the different solvents (NMP and HMPA) allowed to obtain information about the equilibria above mentioned. Where possible K for was calculated (K = [Pd(Rf)(solv)(P-L)$^+$][X$^-$]/[Pd(Rf)X(P-L)]). As an example, Figure ESI8 shows the spectra obtained for [Pd(Rf)I(dppf)] (**3b**).

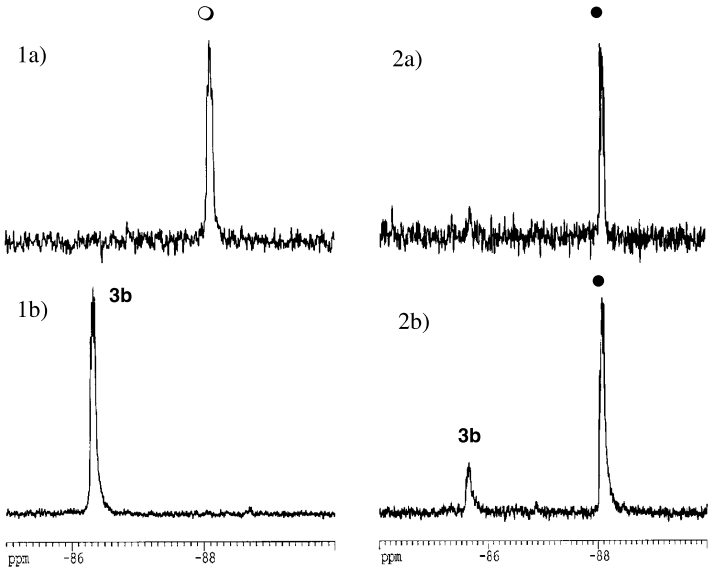

Figure ESI 8. ^{19}F NMR spectra (F^o region) of [Pd(Rf)I(dppf)] (**3b**) in 1) NMP and 2) HMPA at 323 K, a) with $AgBF_4$ and b) without $AgBF_4$ (○ corresponds to the cationic compound [Pd(Rf)(NMP)(dppf)]$^+$ (**7b**$^+$) and ● to the analogous [Pd(Rf)(HMPA)(dppf)]$^+$ (**8b**$^+$).

9. Kinetic details

Kinetic experiments were monitored by ^{19}F NMR. NMR tubes were charged under N_2 with [Pd(Rf)X(P-L)] (X = OTf, I; P-L = dppe, dppf, PPh_2(bzN)) (0.012 mmol), PhC≡C$SnBu_3$ (89 μL, 0.24 mmol) and freshly distilled THF (total volume = 600 μL). α,α,α-Trifluorotoluene (0.020 M) was used as internal standard. Then an acetone-d_6 capillary was added for NMR lock, and placed into a thermostated probe (the temperature was measured by an ethylene glycol standard method).[10] Concentration-time data were then acquired from ^{19}F NMR signal areas of the different species (Figures 5 and 10-14).

During the kinetic experiments some intermediates have been detected and characterised:

[Pd(Rf)(η^2-PhC≡C$SnBu_3$)(dppe)](TfO) (10a). ^{19}F NMR (470.16 MHz, THF/cap. acetone-d_6, 220 K) δ (ppm): –91.10 (br, 2F, F^o), –119.38 (s, 1F, F^p). **^{31}P{^{1}H} NMR** (202.31 MHz, THF/cap. acetone-d_6, 220 K) δ (ppm): 59.3 (br, 1P), 44.4 (br, 1P).

[Pd(η^2-PhC≡CRf)(dppe)] (12a). ^{19}F NMR (470.16 MHz, THF/cap. acetone-d_6, 313 K) δ (ppm) –111.43 (s, 2F, F^o), –121.93 (s, 1F, F^p). **^{31}P{^{1}H} NMR** (202.31 MHz, cap. acetone-d_6, 295 K) δ (ppm): 40.7 (d, $^2J_{P\text{-}P}$ = 32.5 Hz, 1P), 39.5 (d, $^2J_{P\text{-}P}$ = 32.5 Hz, 1P).

[Pd(C≡CPh)($SnBu_3$)(dppe)](14a). **^{31}P{^{1}H} NMR** (202.31 MHz, THF/cap. acetone-d_6, 295 K) δ (ppm) 53.2 (d, $^2J_{P-P}$ = 24.5 Hz, $^2J_{P-Sn}$ = 10.8 Hz, 1P, $P_{cis\text{-}to\text{-}Sn}$), 25.1 (d, $^2J_{P-P}$ = 24.5 Hz, $^2J_{P-^{117}Sn}$ = 1437 Hz; $^2J_{P-^{119}Sn}$ = 1506 Hz, 1P, $P_{trans\text{-}to\text{-}Sn}$).

[Pd(Rf)(C≡CPh)(dppf)] (11b). ^{19}F NMR (470.16 MHz, THF/cap. acetone-d_6, 295 K) δ (ppm) –93.87 (dd, $^4J_{F\text{-}P(trans)}$ = 13.8 Hz, $^4J_{F\text{-}P(cis)}$ = 7.8 Hz, 2F, F^o), –123.00 (s, 1F, F^p). **^{31}P{^{1}H} NMR** (202.31 MHz, THF/cap. acetone-d_6, 295 K) δ (ppm) 16.5 (m, 1P), 15.3 (m, 1P).

[Pd(η^2-RfC≡CPh)(dppf)] (12b). ^{19}F NMR (470.16 MHz, THF/cap. acetone-d_6, 295 K) δ (ppm) –112,20 (s, 2F, F^o), –122.16 (s, 1F, F^p). **^{31}P{^{1}H} NMR** (202.31 MHz, THF/cap. acetone-d_6, 295 K) δ (ppm) 22.2 (m, 1P), 21.2 (m, 1P).

[Pd(Rf)(C≡CPh){PPh_2(bzN)}] (11c). ^{19}F NMR (470.16 MHz, THF/cap. acetone-d_6, 313 K) δ (ppm): –87.32 (vbr, 2F, F^o), –123.95 (d, $^6J_{F\text{-}P}$ = 2.7 Hz, 1F, F^p). **^{31}P{^{1}H} NMR** (202.31 MHz, THF/cap. acetone-d_6, 295 K) δ (ppm) 19.0 (br, 1P).

[Pd(C≡CPh)($SnBu_3$){PPh_2(bzN)}] (14c). **^{31}P{^{1}H} NMR** (202.31 MHz, THF/cap. acetone-d_6, 295 K) δ (ppm) 28.64 (s, $^2J_{P-Sn}$ = 15.0 Hz, 1P). See Figure ESI9.

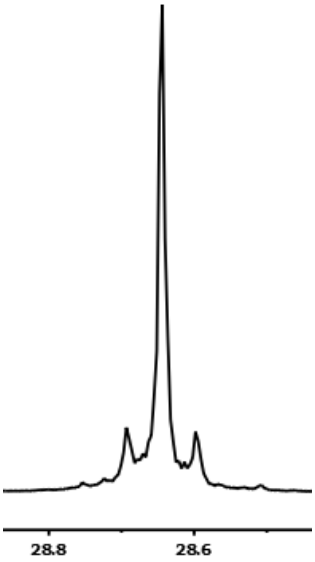

Figure ESI 9. $^{31}P\{^{1}H\}$ NMR spectra of [Pd(C≡CPh)($SnBu_3$){PPh_2(bzN)}] (**14c**).

Kinetic simulations with COPASI Software

The kinetic models were fitted to the measured concentration *vs.* time experimental data by nonlinear least-squares (NLLS) regression, using the software COPASI.[12] Tables ESI4 and ESI5 summarise the adjusted kinetic constants for the data depicted in Figures 5 and 10 respectively, with the corresponding kinetic equations (Schemes ESI1 and ESI2). Some of the rate constants of reversible processes involving experimentally unobservable species (for example intermediate **10a**), were fixed to be sufficiently high, taking into account their extremely fast evolution in the conditions of our monitoring. In these cases, equilibrium constants ($K_{eq} = k_n / k_{-n}$) are crucial, as happen in the pre equilibria forming **10a**(X). With X = OTf, $k_1 > k_{-1}$, while with X = I; $k_1 << k_{-1}$.

The competitive reactions from **11a** were adjusted with the experimental data. Standard deviations for the fitted rate constants are given in the Tables below.

The units of the rate constants are (s^{-1}) or (mol^{-1} L s^{-1}) for first and second order kinetic reactions respectively.

*a) Reaction of [Pd(Rf)(OTf)(dppe)] (**4a**) with PhC≡CSnBu$_3$ (**9**) in THF*

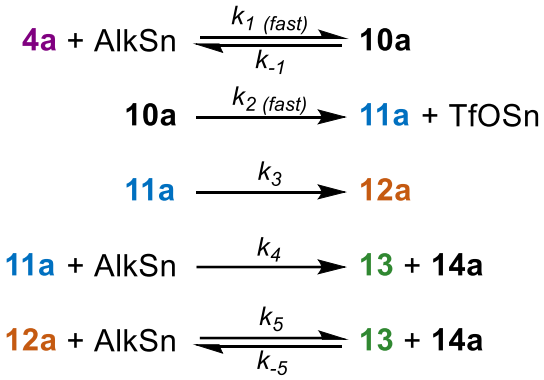

Scheme ESI 1. Kinetic equations for the fitting of Figure 5 (PhC≡CSnBu$_3$ denoted as AlkSn) .

Table ESI 4. Fitted rate constants. Starting conditions [**4a**]$_0$ = 0.02 mol L^{-1}, [**9**]$_0$ = 0.4 mol L^{-1}.

k_1	5.01×10^{-1}
k_{-1}	4.03×10^{-5}
k_2	1.01
k_3	$(2.63 \pm 0.07) \times 10^{-5}$
k_4	$(1.26 \pm 0.03) \times 10^{-4}$
k_5	9.58×10^{-5}
k_{-5}	2.66×10^{-4}

*b) Reaction of [Pd(Rf)I(dppe)] (**3a**) with PhC≡CSnBu$_3$ (**9**) in THF*

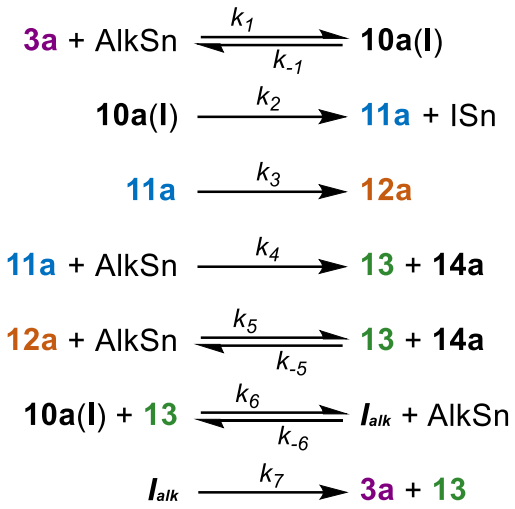

Scheme ESI 2. Kinetic equations for the fitting of Figure 10. *$\boldsymbol{I_{alk}}$ is the species formed after the ligand substitution of η^2-PhC≡CSnBu$_3$ by PhC≡CRf.

Table ESI 5. Fitted rate constants. Starting conditions [**3a**]$_0$ = 0.02 mol L^{-1}, [**9**]$_0$ = 0.4 mol L^{-1}.

$\boldsymbol{k_1}$	9.18
$\boldsymbol{k_{-1}}$	10^4
$\boldsymbol{k_2}$	5.59×10^{-1}
$\boldsymbol{k_3}$	$(2.11 \pm 0.02) \times 10^{-5}$
$\boldsymbol{k_4}$	$(1.29 \pm 0.02) \times 10^{-4}$
$\boldsymbol{k_5}$	10^{-6}
$\boldsymbol{k_{-5}}$	10^{-8}
$\boldsymbol{k_6}$	3.00×10^7
$\boldsymbol{k_{-6}}$	3.69×10^{-2}
$\boldsymbol{k_7}$	10^4

10. Computational Section

Density functional theory (DFT) calculations reported in this work were carried out using the dispersion corrected hybrid functional ωB97X-D developed by Head-Gordon and Chai,[13] and the Gaussian09 software.[14] The choice of this level of theory is based on the satisfactory results obtained in previous theoretical studies on Pd/Sn[15] transmetalations. C, P and H atoms were described using the double-ζ basis set 6-31G(d,p), whereas the same basis set plus diffuse functions was employed to describe the more electronegative Cl and F atoms. Pd and Sn were described using the effective core potential LANL2DZ[16] including f-polarization functions (exponent: 1.472 for Pd and 0.180 for Sn).[17] The geometry optimizations were performed in THF (SMD solvation model)[18] without imposing any constraint and the nature of the stationary point was further verified through vibrational frequency analysis. To simplify the calculations, $SnBu_3$ group was reduce to $SnMe_3$. Selected interactions for [Pd(Rf)(η^2-PhC≡C$SnMe_3$)(dppe)]$^+$ (**10a**$^+$), were analysed by means of Natural Bond Orbital (NBO) and Second Order Perturbation Theory (SOPT).[19] The Donor-Acceptor Interactions collected in Table 4 are shown in Figure ESI10.

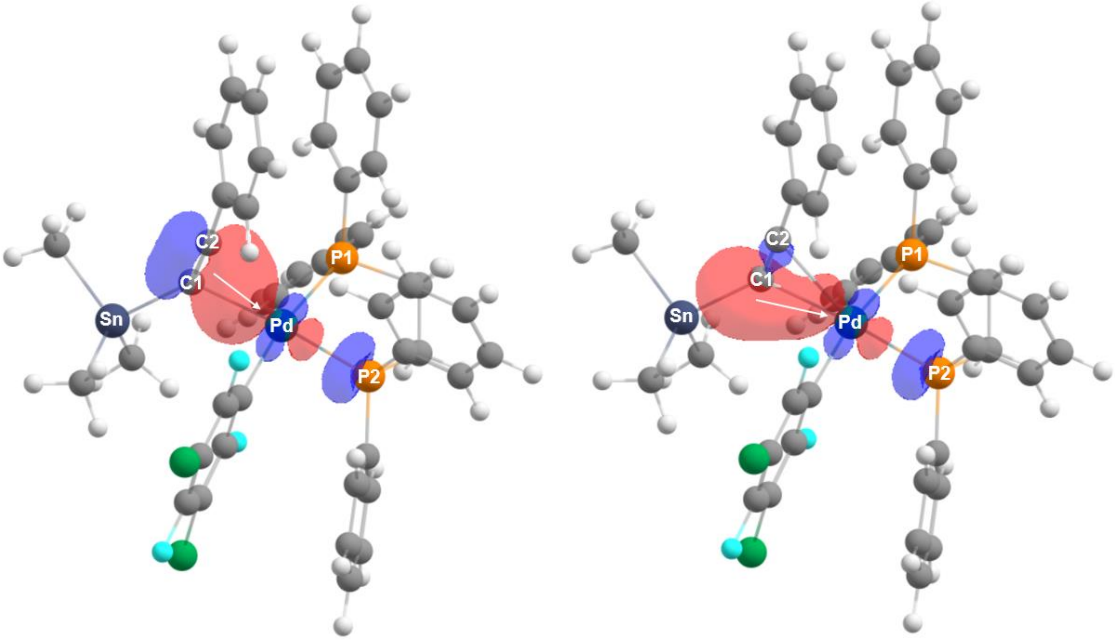

Figure ESI 10. Pictorial view of the NBO interactions summarised in Table 4. Donors: **BD C1-C2** (left) and **BD C1-Sn** (right). Common Acceptor: **BD* Pd-P2**.

Cartesian coordinates of $[Pd(Rf)(\eta^2\text{-}PhC{\equiv}CSnMe_3)(dppe)]^+$ (**10a**$^+$)

46	0.242267000	0.088506000	0.212492000
15	-0.357644000	2.000929000	1.311817000
15	2.271613000	0.316747000	1.428339000
17	-4.092366000	1.182639000	-3.441833000
17	-5.142274000	-1.298904000	1.255153000
9	-1.327463000	1.081335000	-2.467345000
9	-2.238510000	-1.063758000	1.610797000
9	-5.740541000	-0.067159000	-1.352047000
6	-2.089414000	2.280805000	1.748929000
6	2.364094000	-0.989138000	2.690840000
6	-1.707064000	-0.010054000	-0.421414000
6	-3.542404000	0.505647000	-1.954843000
6	0.178686000	3.443933000	0.345145000
6	2.390441000	-2.925308000	4.701201000
1	2.400920000	-3.676790000	5.483576000
6	-2.193319000	0.508495000	-1.605675000
6	0.631121000	-1.796450000	-0.988080000
6	0.668672000	2.089033000	2.843166000
1	0.527616000	3.054812000	3.336823000
1	0.335212000	1.301863000	3.526920000
6	3.903218000	0.445481000	0.636772000
6	-3.990530000	1.836225000	3.167569000
1	-4.404404000	1.411288000	4.075383000
6	-0.044431000	4.736622000	0.835432000
1	-0.598002000	4.885434000	1.758454000
6	-2.653950000	-0.558140000	0.427231000
6	2.367924000	-0.429735000	-2.478182000
6	-2.929500000	2.915020000	0.825754000
1	-2.522181000	3.331945000	-0.090214000
6	-4.824620000	2.463077000	2.245695000
1	-5.890559000	2.527753000	2.435997000
6	-2.625152000	1.739056000	2.920452000
1	-1.992786000	1.217926000	3.632076000
6	-4.444937000	-0.054233000	-1.054835000
6	2.128365000	1.869716000	2.440168000
1	2.775314000	1.798541000	3.318058000
1	2.483656000	2.707221000	1.832725000
6	3.366290000	-0.976091000	3.670758000
1	4.144480000	-0.217972000	3.649375000
6	-4.016181000	-0.601223000	0.152375000
6	0.430142000	5.837051000	0.131628000
1	0.254857000	6.836927000	0.513843000
6	-4.293355000	3.003564000	1.076375000
1	-4.941887000	3.491618000	0.356677000
6	0.871133000	3.269667000	-0.855447000
1	1.036012000	2.269864000	-1.245290000
6	3.380543000	-1.943844000	4.667084000
1	4.161308000	-1.931985000	5.419973000
6	1.431158000	-1.138793000	-1.665163000
6	1.126954000	5.656365000	-1.062710000
1	1.494014000	6.519093000	-1.608666000
6	1.389960000	-2.941488000	3.735163000
1	0.614386000	-3.699765000	3.761562000
6	4.184301000	0.911357000	-4.102902000
1	4.892138000	1.432424000	-4.739369000
6	1.345902000	4.374180000	-1.556856000
1	1.879704000	4.226911000	-2.490076000
6	3.700004000	-0.861213000	-2.543819000
1	4.017126000	-1.712117000	-1.951692000
6	1.946244000	0.671751000	-3.240143000
1	0.905261000	0.974369000	-3.205182000
6	4.858662000	-0.568564000	0.739577000
1	4.643316000	-1.467989000	1.307353000
6	2.860065000	1.343725000	-4.040422000
1	2.534742000	2.190690000	-4.635611000
6	6.100006000	-0.420276000	0.125444000
1	6.842739000	-1.205591000	0.219620000
6	6.390844000	0.733703000	-0.594461000
1	7.362844000	0.852019000	-1.062004000
6	4.189246000	1.590771000	-0.117359000
1	3.444043000	2.372467000	-0.240186000
6	4.599903000	-0.192714000	-3.361790000
1	5.629620000	-0.528415000	-3.414924000
6	5.430489000	1.735247000	-0.722442000
1	5.647419000	2.629191000	-1.297323000
50	-0.582146000	-3.576295000	-0.990782000
6	-2.315839000	-3.087578000	-2.126682000
1	-2.717480000	-3.986469000	-2.600866000
1	-2.058272000	-2.367701000	-2.906999000
1	-3.090920000	-2.654568000	-1.491600000
6	0.689362000	-4.971815000	-1.981228000
1	0.933193000	-4.613147000	-2.984110000
1	1.619339000	-5.108183000	-1.424225000
1	0.196308000	-5.942938000	-2.073046000
6	-0.969437000	-4.142089000	1.024224000
1	-1.649809000	-4.997538000	1.040965000
1	-0.038269000	-4.436151000	1.515006000
1	-1.433202000	-3.324961000	1.580514000
6	1.377496000	-1.978730000	2.729198000
1	0.596611000	-1.997124000	1.975151000

Cartesian coordinates of $[Pd(Rf)(THF)(dppe)]^+$ (**6a**$^+$)

46	-0.427527000	-0.212243000	0.189729000	1	-1.409625000	-2.528488000	-1.065431000
15	-2.527643000	0.146296000	-0.783183000	6	1.948322000	0.685031000	-2.164810000
15	0.323434000	1.096231000	-1.479790000	6	2.076880000	-0.337291000	-3.109823000
9	1.584978000	-2.451634000	-0.610900000	1	1.200895000	-0.829384000	-3.521125000
9	5.560402000	-1.182858000	1.536829000	6	3.342538000	-0.747984000	-3.518078000
9	1.640457000	1.310828000	2.215257000	1	3.438328000	-1.538191000	-4.255635000
6	-2.316570000	1.322104000	-2.191811000	6	4.479951000	-0.152403000	-2.977729000
1	-3.118156000	1.182716000	-2.921633000	1	5.465367000	-0.480743000	-3.293030000
1	-2.380368000	2.344666000	-1.809031000	6	4.353794000	0.863396000	-2.031612000
6	-0.943299000	1.068791000	-2.822435000	1	5.237745000	1.328487000	-1.607351000
1	-0.696657000	1.827551000	-3.570366000	6	3.092560000	1.283956000	-1.624577000
1	-0.915310000	0.087051000	-3.304943000	1	3.003074000	2.070450000	-0.881471000
6	1.523122000	-0.556757000	0.786986000	6	0.362919000	2.834111000	-0.956737000
6	2.229110000	-1.609861000	0.230063000	6	0.846189000	3.811222000	-1.835816000
6	3.579619000	-1.855684000	0.455955000	1	1.269417000	3.526174000	-2.794980000
6	4.259687000	-0.986265000	1.301045000	6	0.793431000	5.152850000	-1.476086000
6	3.608493000	0.081115000	1.907307000	1	1.171386000	5.907579000	-2.158076000
6	2.253816000	0.256855000	1.631778000	6	0.255198000	5.526127000	-0.244888000
6	-3.785466000	0.787214000	0.356625000	1	0.213735000	6.575186000	0.030714000
6	-4.627445000	-0.101055000	1.035671000	6	-0.226979000	4.557634000	0.630995000
1	-4.611240000	-1.160773000	0.800327000	1	-0.643368000	4.845721000	1.590784000
6	-5.488528000	0.371791000	2.021775000	6	-0.173265000	3.211509000	0.277709000
1	-6.140985000	-0.321903000	2.542269000	1	-0.542292000	2.453590000	0.963301000
6	-5.513161000	1.727927000	2.337857000	17	4.472706000	1.154883000	2.954020000
1	-6.188154000	2.094582000	3.104634000	17	4.403902000	-3.182133000	-0.287843000
6	-4.671096000	2.614025000	1.668778000	6	-1.580205000	-0.634696000	3.039791000
1	-4.687925000	3.671791000	1.911331000	8	-1.330259000	-1.336444000	1.804021000
6	-3.803555000	2.148051000	0.685940000	6	-1.018780000	-2.726588000	2.075091000
1	-3.140797000	2.850534000	0.188596000	6	-1.309454000	-2.927685000	3.565124000
6	-3.179111000	-1.378752000	-1.523333000	6	-2.162875000	-1.708163000	3.937557000
6	-4.443976000	-1.395114000	-2.124776000	1	-0.634694000	-0.239972000	3.431339000
1	-5.059554000	-0.499575000	-2.127928000	1	-2.258906000	0.189477000	2.810890000
6	-4.918149000	-2.562506000	-2.711174000	1	-1.664029000	-3.323771000	1.425943000
1	-5.899284000	-2.573102000	-3.174659000	1	0.027846000	-2.910675000	1.819316000
6	-4.134661000	-3.716885000	-2.704238000	1	-1.818365000	-3.874771000	3.752283000
1	-4.509785000	-4.626439000	-3.162639000	1	-0.376293000	-2.921023000	4.135224000
6	-2.874938000	-3.704361000	-2.112951000	1	-3.215944000	-1.872215000	3.688629000
1	-2.263197000	-4.600871000	-2.109600000	1	-2.087563000	-1.447874000	4.994910000
6	-2.395570000	-2.537110000	-1.522396000				

Cartesian coordinates of PhC≡CSnMe$_3$

6	2.686732000	-0.000066000	-0.020610000	50	-2.078219000	0.000034000	0.000565000
6	0.032568000	-0.000102000	-0.037596000	6	-2.723655000	-1.772748000	-1.001969000
6	1.252001000	-0.000108000	-0.032423000	1	-2.249289000	-2.654124000	-0.561386000
6	3.395009000	1.211089000	-0.012069000	1	-3.808575000	-1.882568000	-0.913685000
1	2.848689000	2.148877000	-0.018324000	1	-2.463726000	-1.729027000	-2.063358000
6	3.395098000	-1.211171000	-0.012374000	6	-2.651489000	0.002280000	2.059292000
1	2.848848000	-2.148999000	-0.018863000	1	-2.260965000	-0.885832000	2.563937000
6	5.482989000	0.000033000	0.014666000	1	-2.259373000	0.890487000	2.562532000
1	6.568636000	0.000072000	0.029564000	1	-3.741813000	0.003336000	2.149841000
6	4.785204000	1.206450000	0.005652000	6	-2.723320000	1.770502000	-1.006278000
1	5.325060000	2.148257000	0.012968000	1	-3.808193000	1.880883000	-0.918138000
6	4.785293000	-1.206434000	0.005350000	1	-2.248600000	2.652853000	-0.568041000
1	5.325220000	-2.148202000	0.012432000	1	-2.463538000	1.723929000	-2.067579000

11. NMR spectra

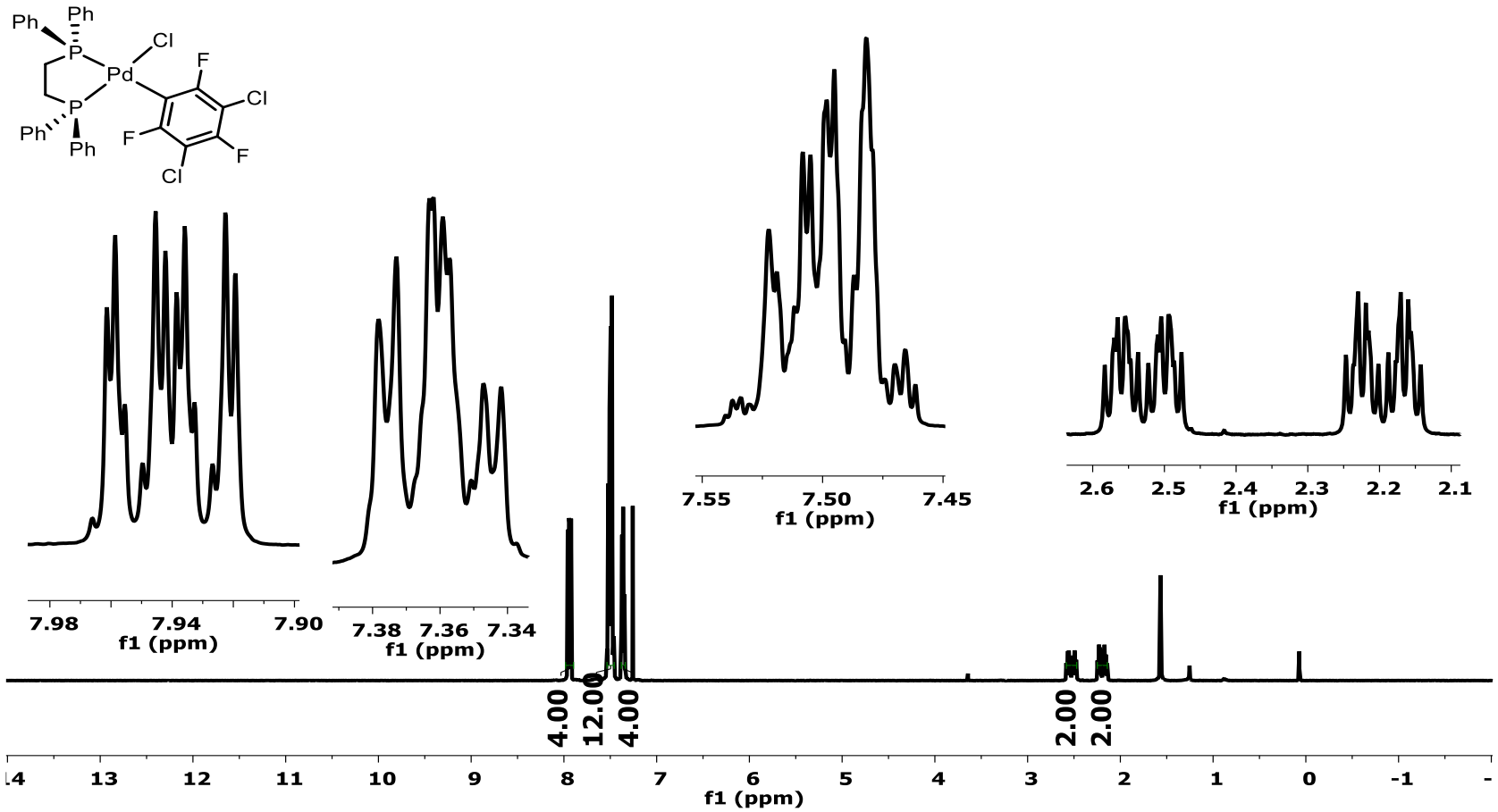

Figure ESI 11. ^{1}H NMR (500 MHz, $CDCl_3$, 298 K) of **2a**

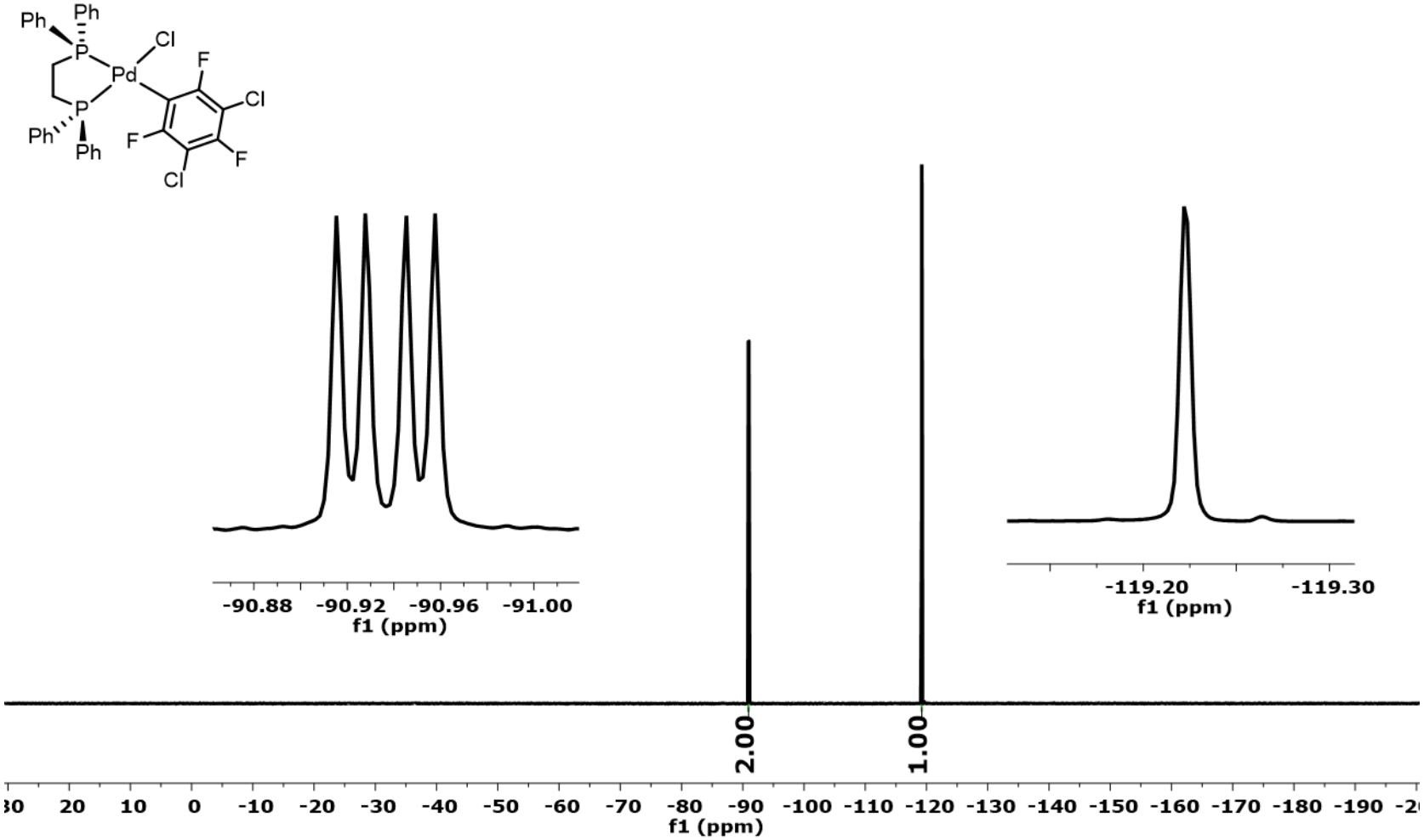

Figure ESI 12. ^{19}F NMR (470 MHz, $CDCl_3$, 298 K) of **2a**

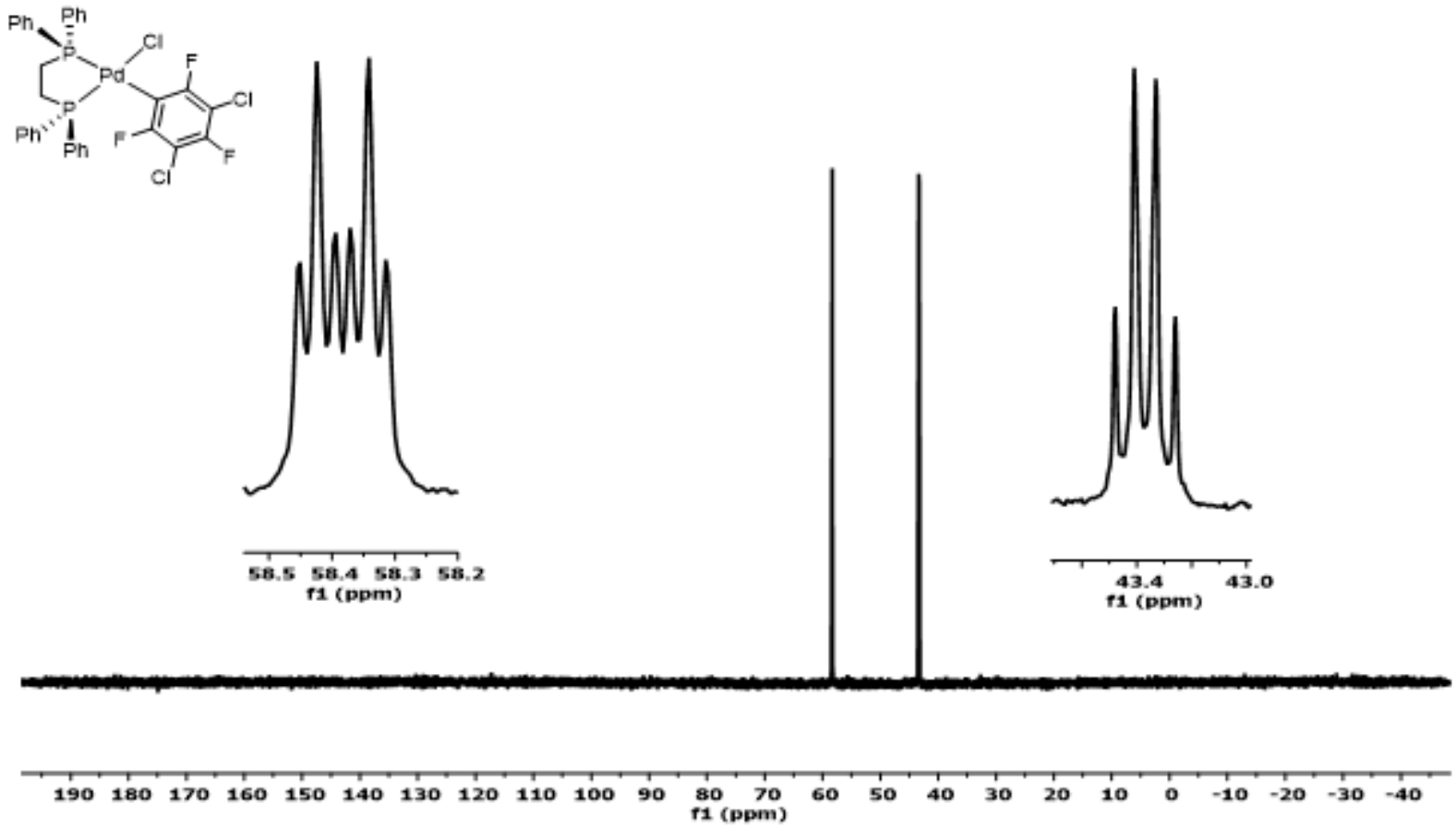

Figure ESI 13. $^{31}P\{^{1}H\}$ NMR (202 MHz, $CDCl_3$, 298 K) of **2a**

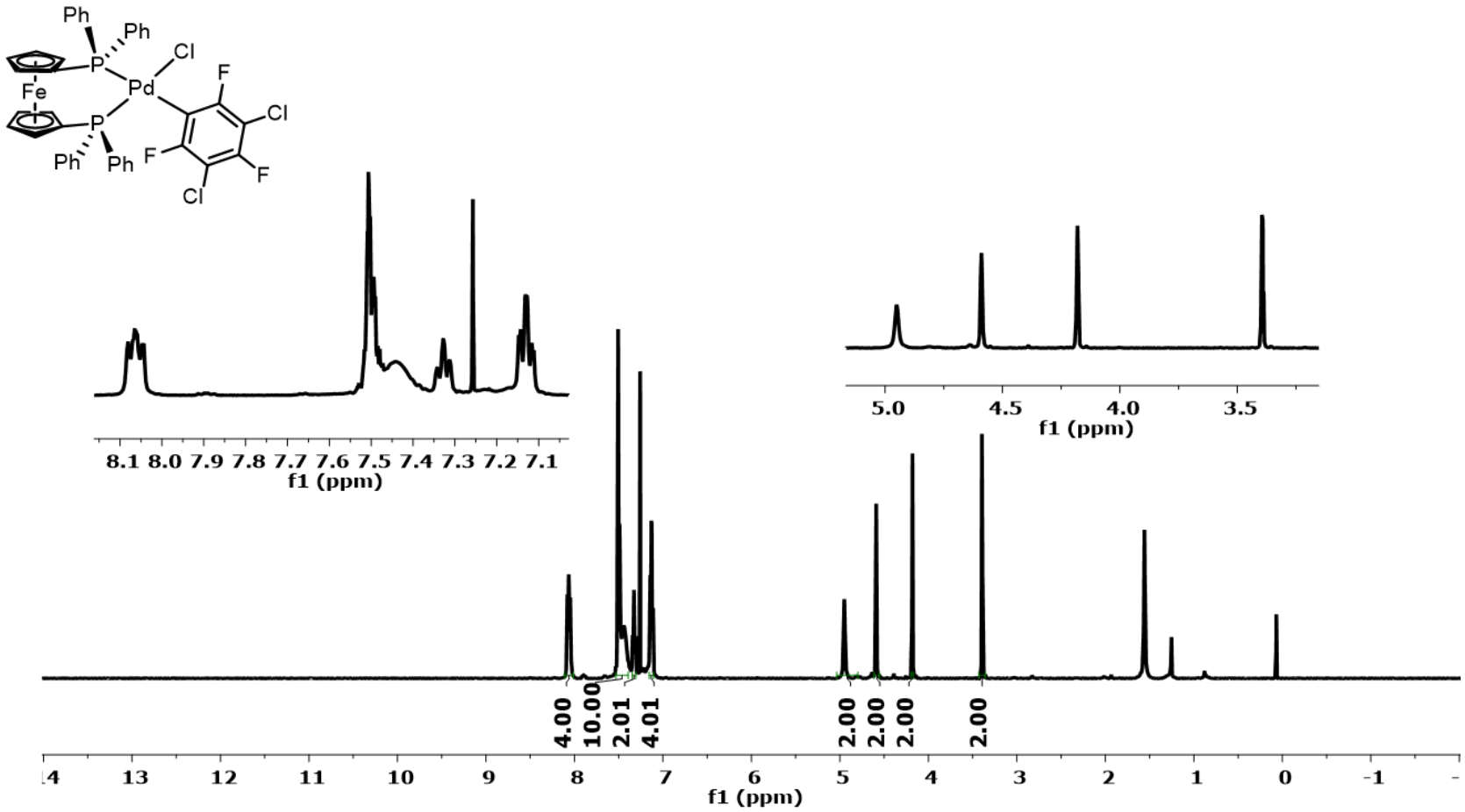

Figure ESI 14. ^{1}H NMR (500 MHz, $CDCl_3$, 298 K) of **2b**

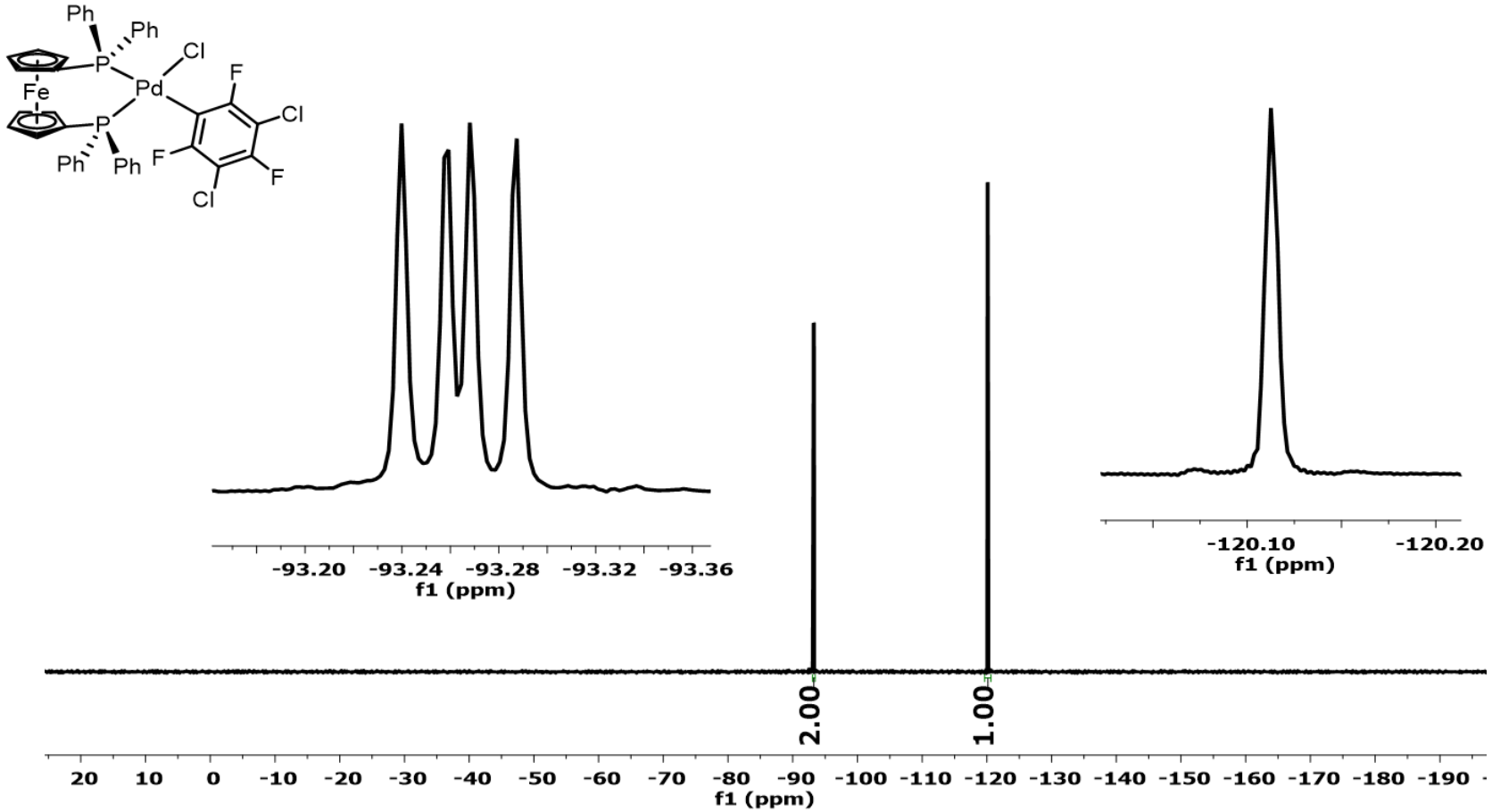

Figure ESI 15. ^{19}F NMR (470 MHz, $CDCl_3$, 298 K) of **2b**

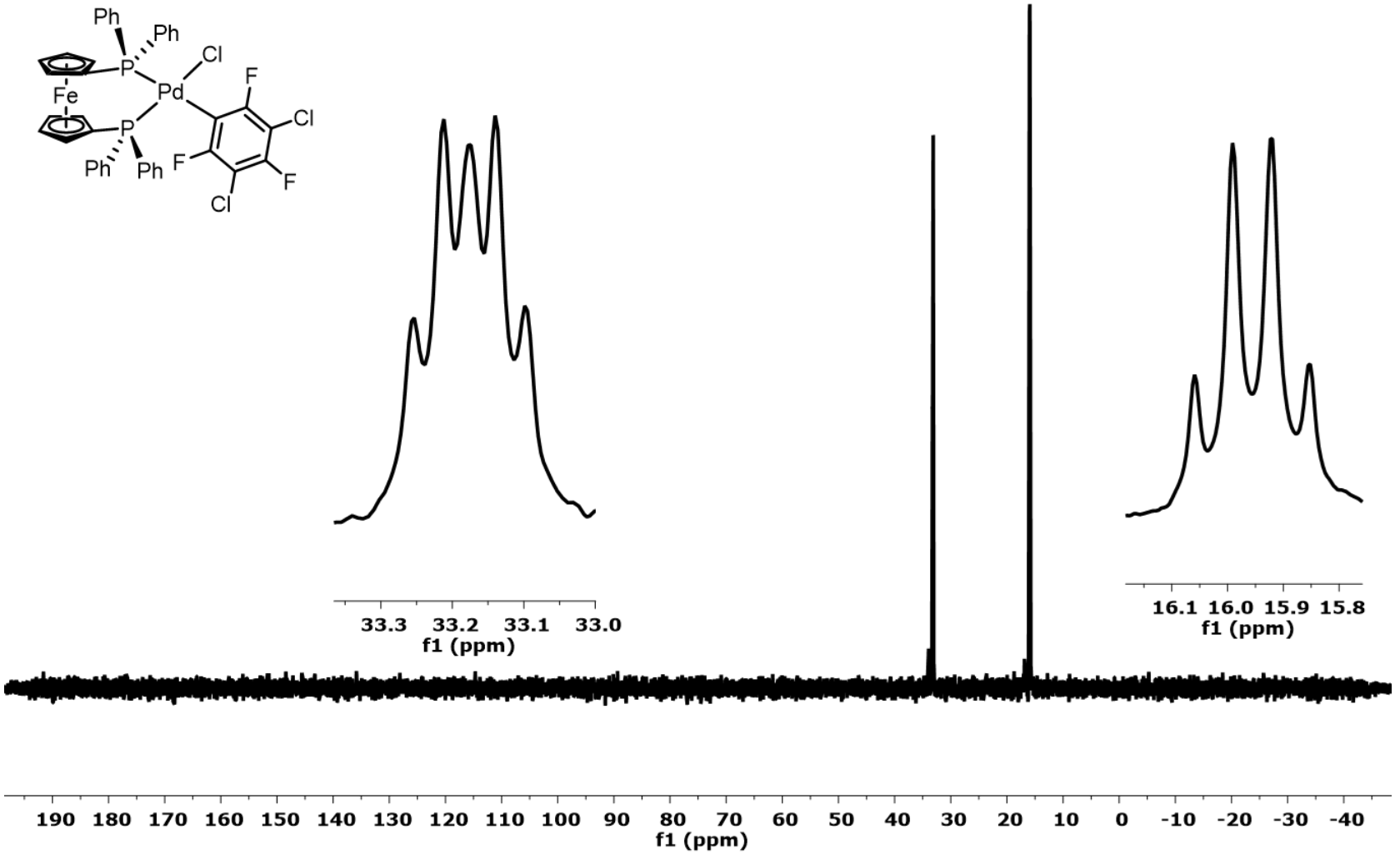

Figure ESI 16. $^{31}P\{^{1}H\}$ NMR (202 MHz, $CDCl_3$, 298 K) of **2b**

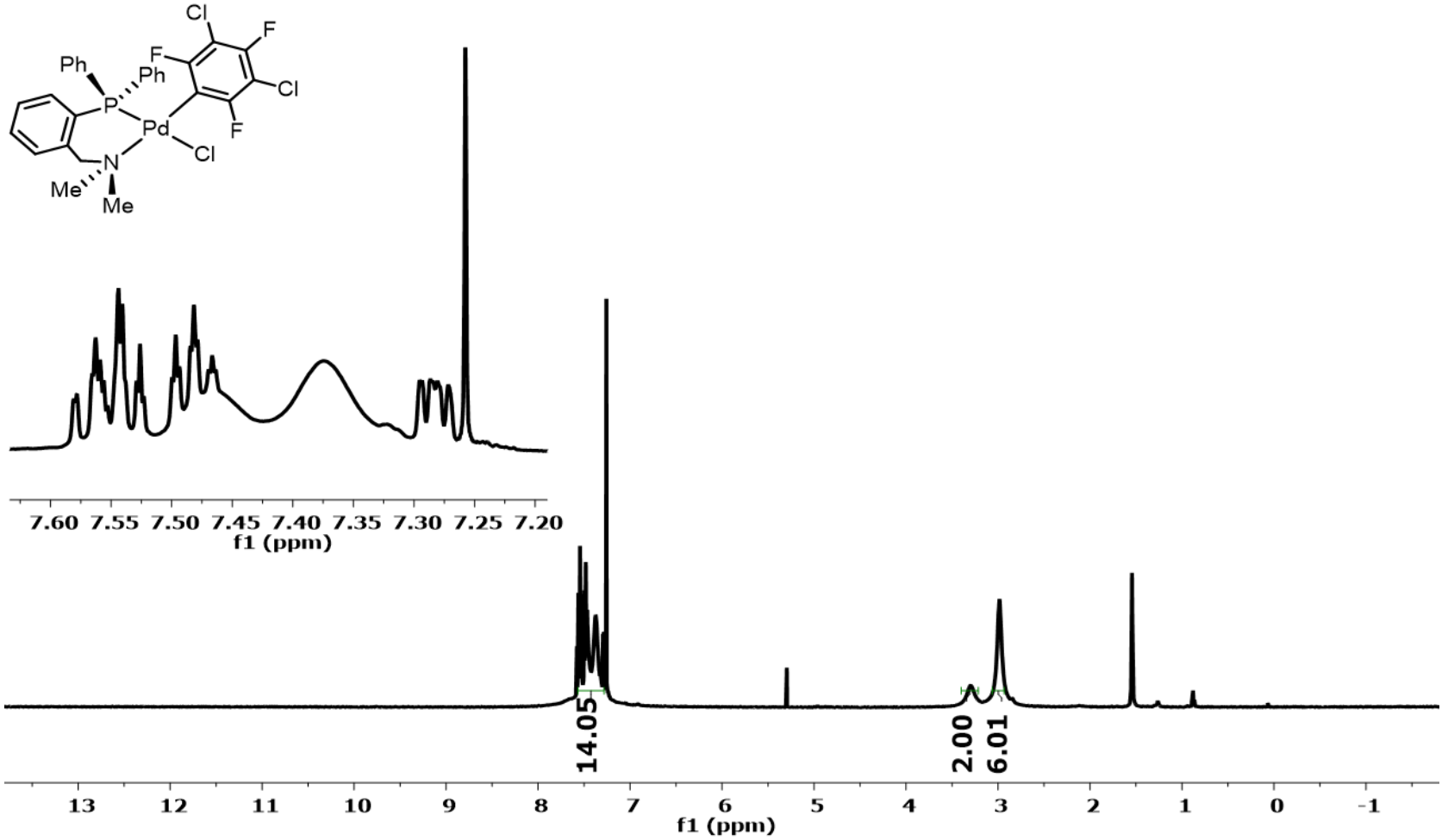

Figure ESI 17. ^{1}H NMR (500 MHz, $CDCl_3$, 298 K) of **2c**

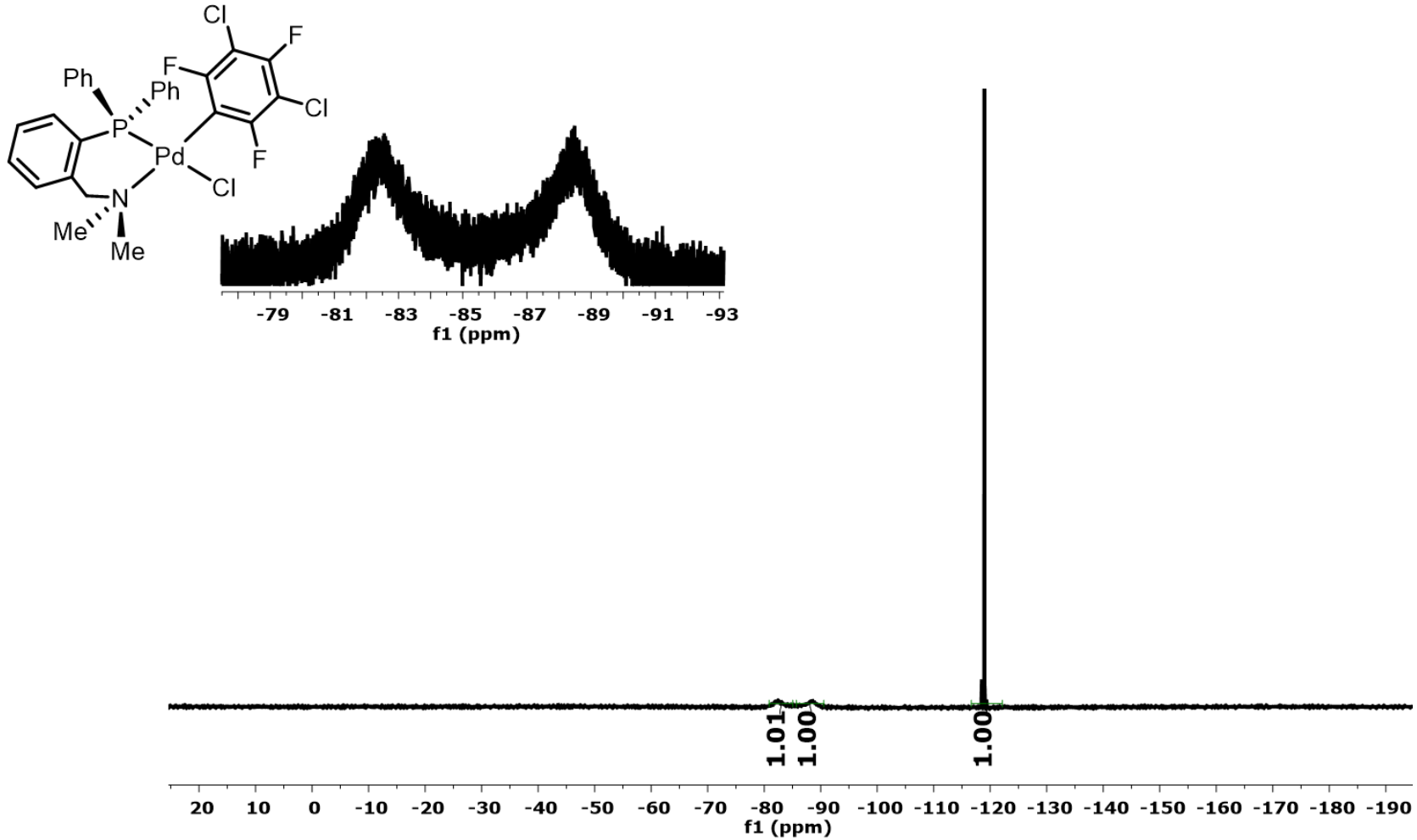

Figure ESI 18. ^{19}F NMR (470 MHz, $CDCl_3$, 298 K) of **2c**

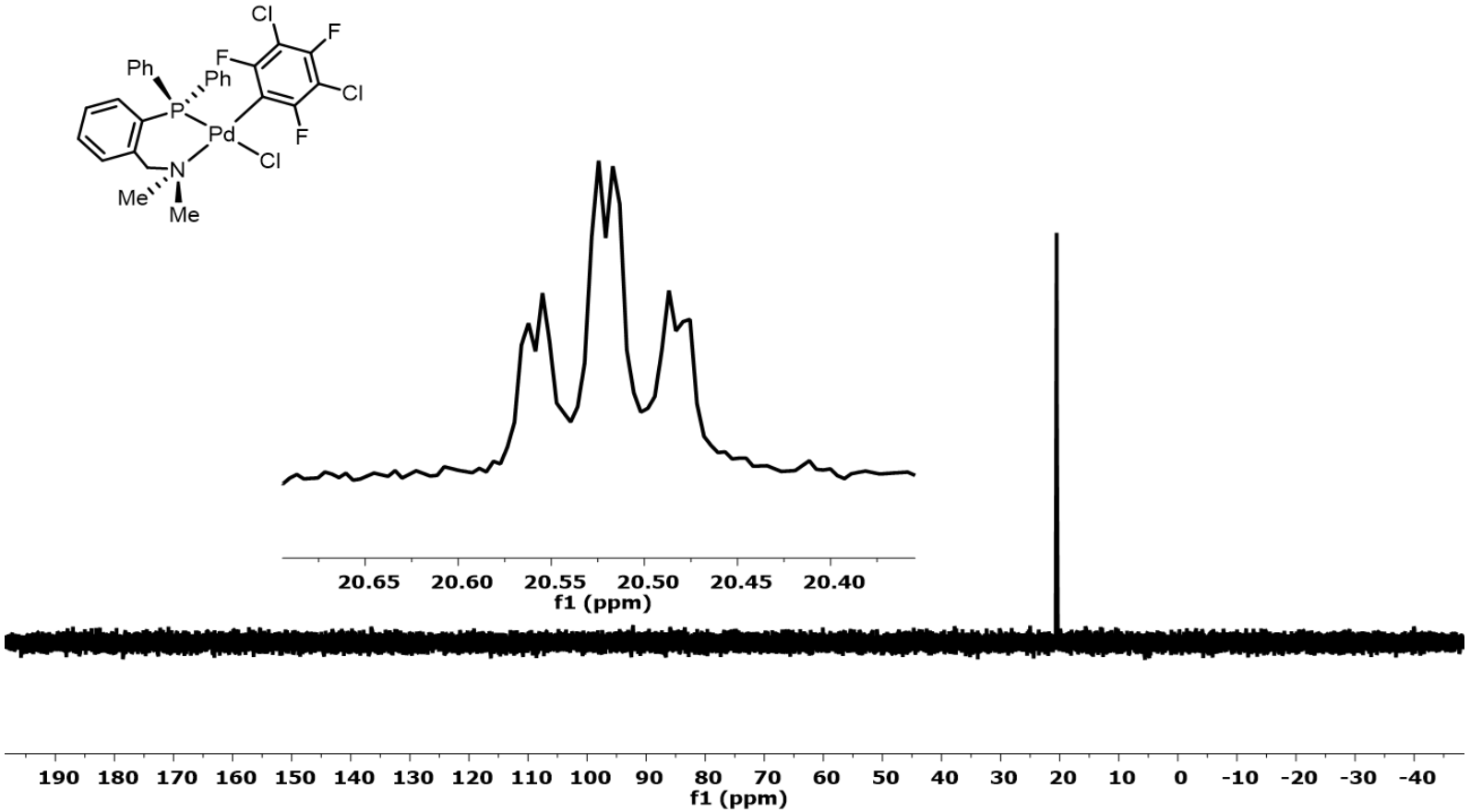

Figure ESI 19. $^{31}P\{^{1}H\}$ NMR (202 MHz, $CDCl_3$, 298 K) of **2c**

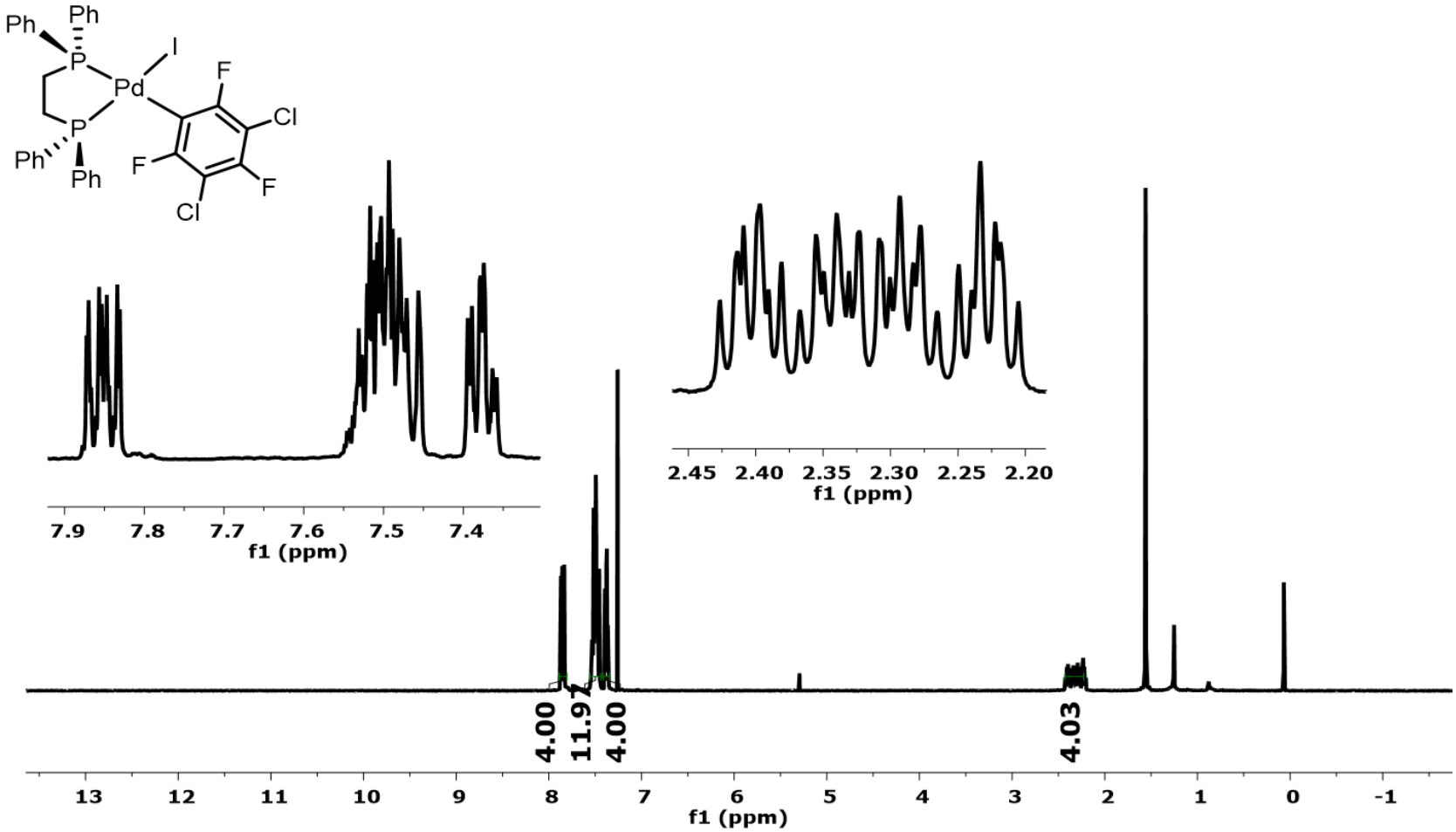

Figure ESI 20. ^{1}H NMR (500 MHz, $CDCl_3$, 298 K) of **3a**

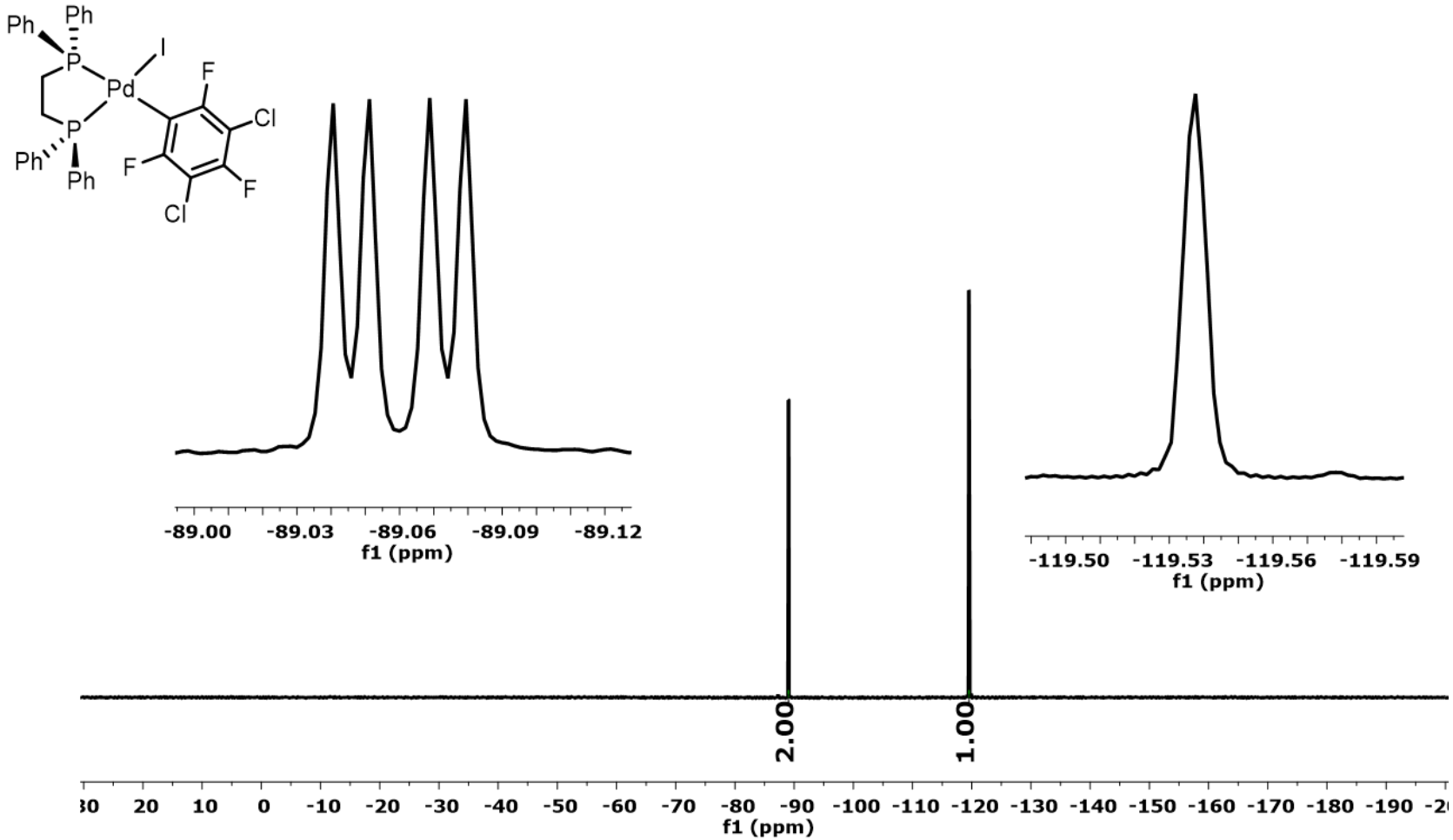

Figure ESI 21. ^{19}F NMR (470 MHz, $CDCl_3$, 298 K) of **3a**

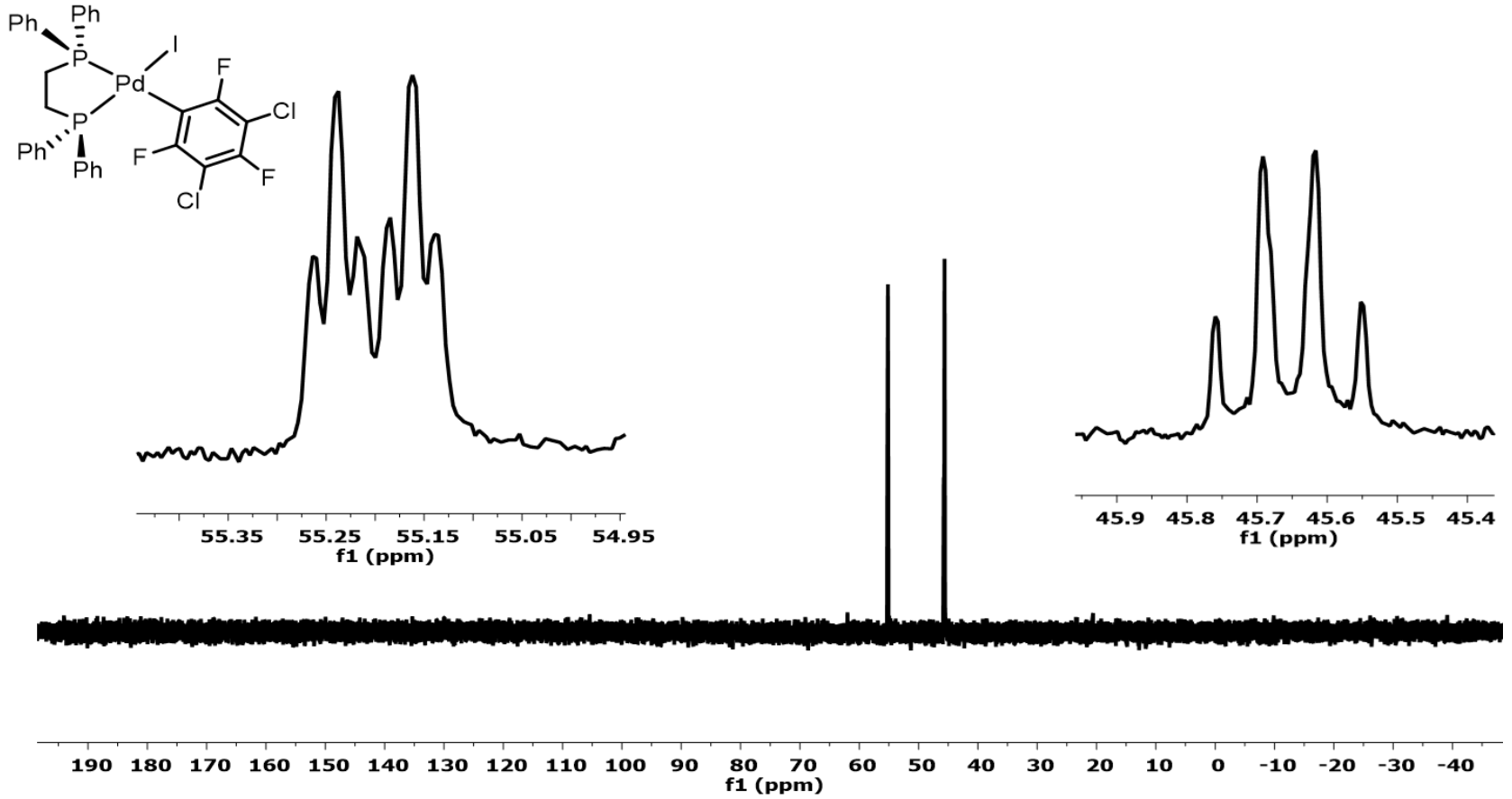

Figure ESI 22. $^{31}P\{^{1}H\}$ NMR (202 MHz, $CDCl_3$, 298 K) of **3a**

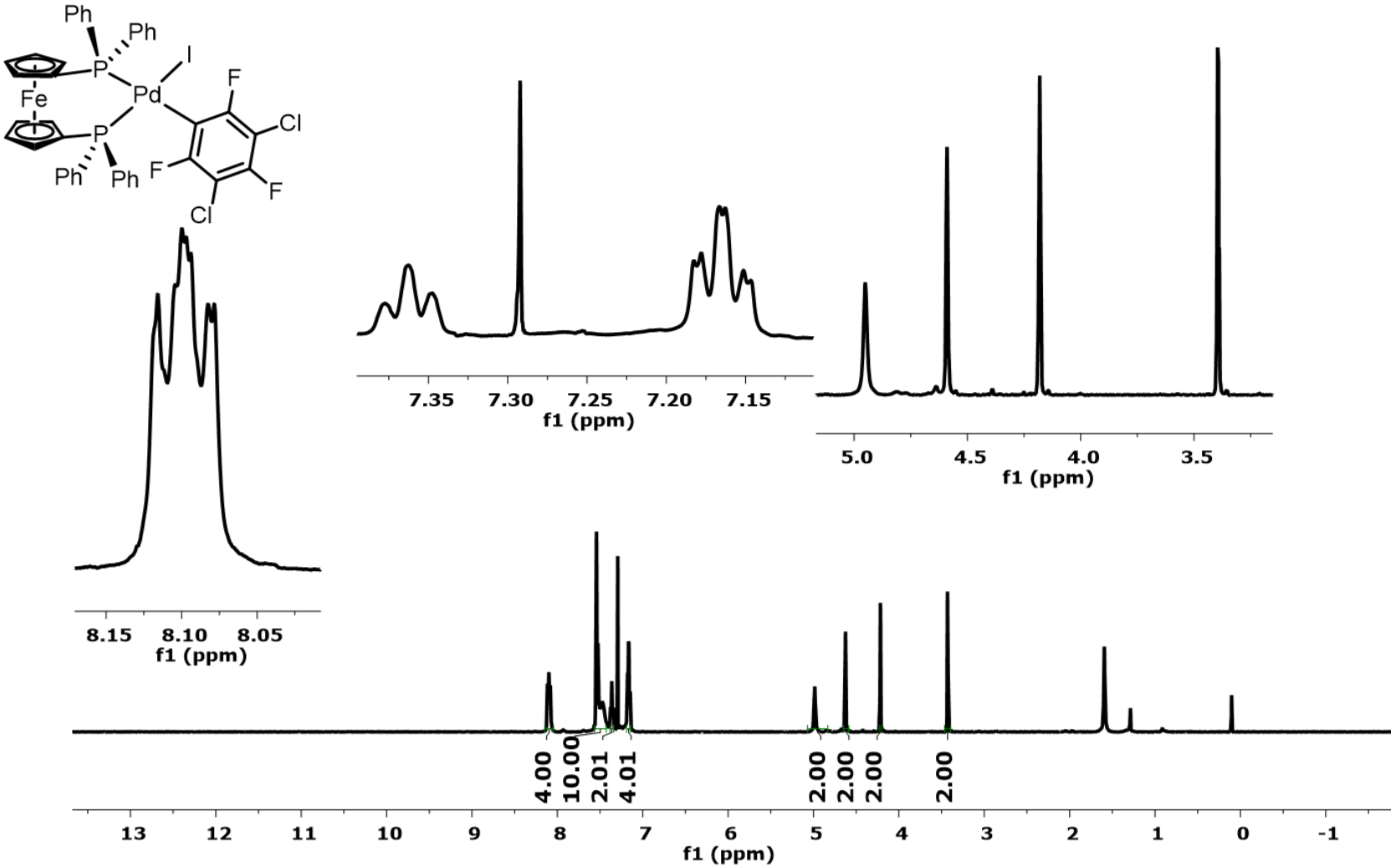

Figure ESI 23. ^{1}H NMR (400 MHz, $CDCl_3$, 298 K) of **3b**

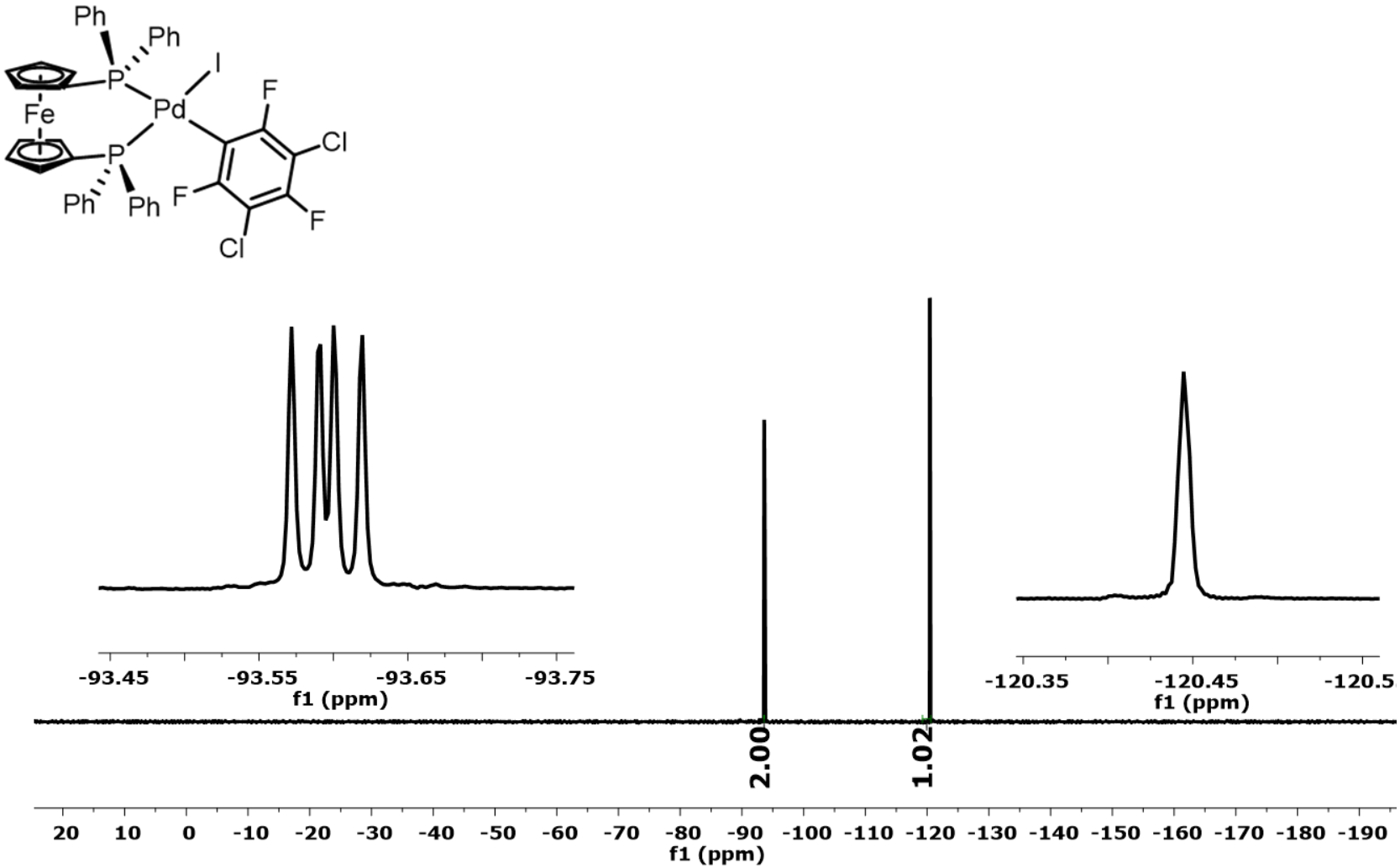

Figure ESI 24. ^{19}F NMR (376 MHz, $CDCl_3$, 298 K) of **3b**

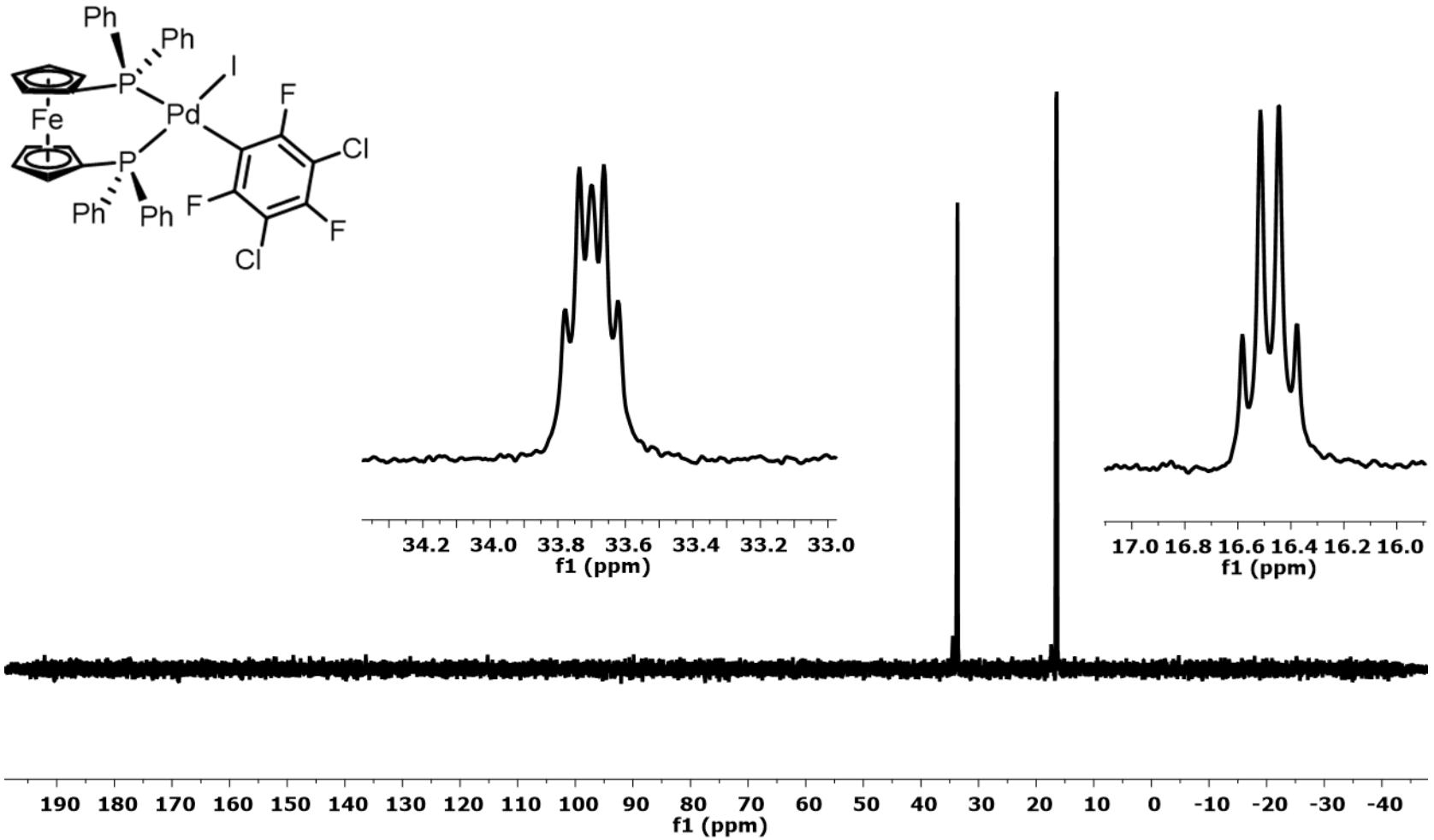

Figure ESI 25. $^{31}P\{^{1}H\}$ NMR (162 MHz, $CDCl_3$, 298 K) of **3b**

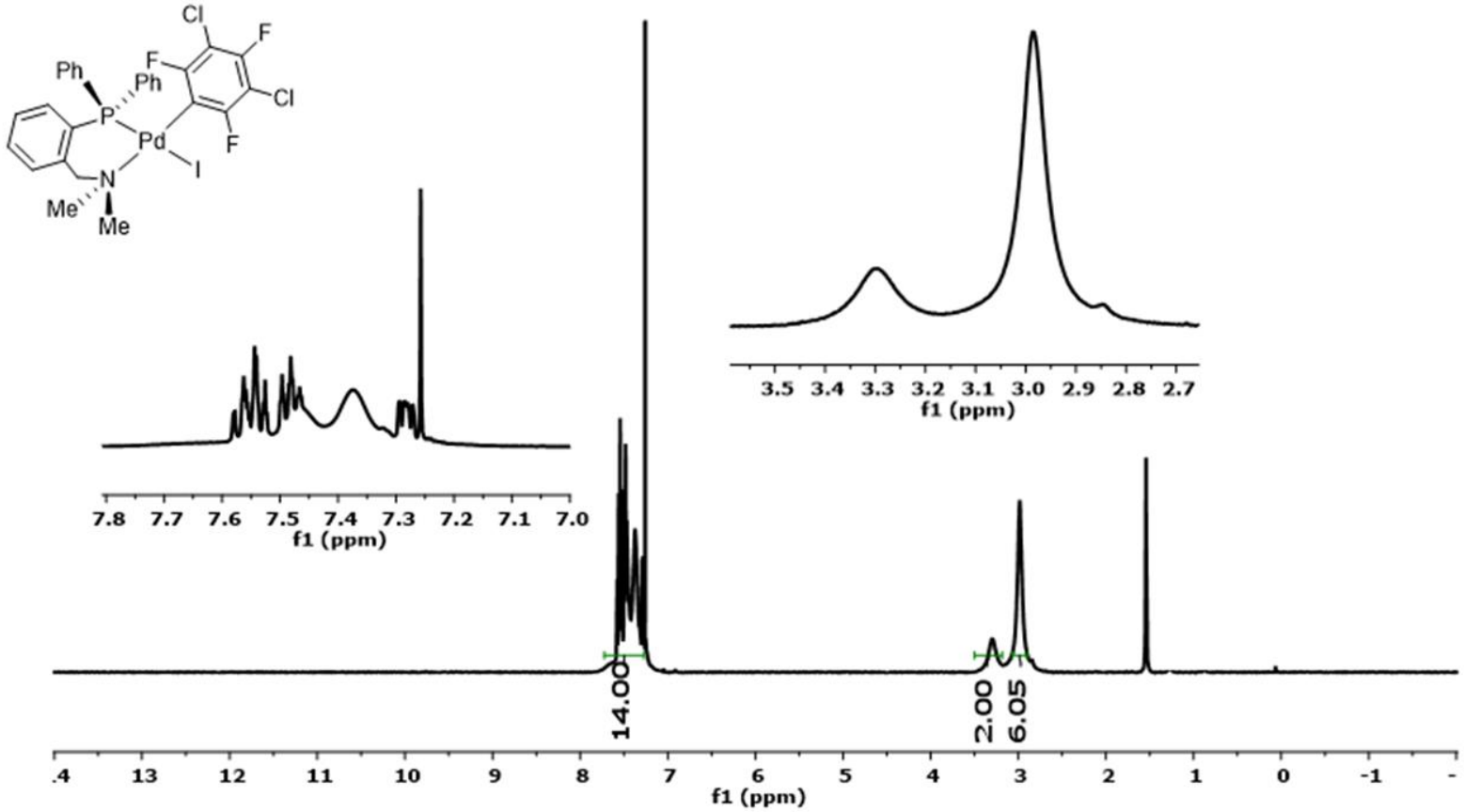

Figure ESI 26. ^{1}H NMR (500 MHz, $CDCl_3$, 298 K) of **3c**

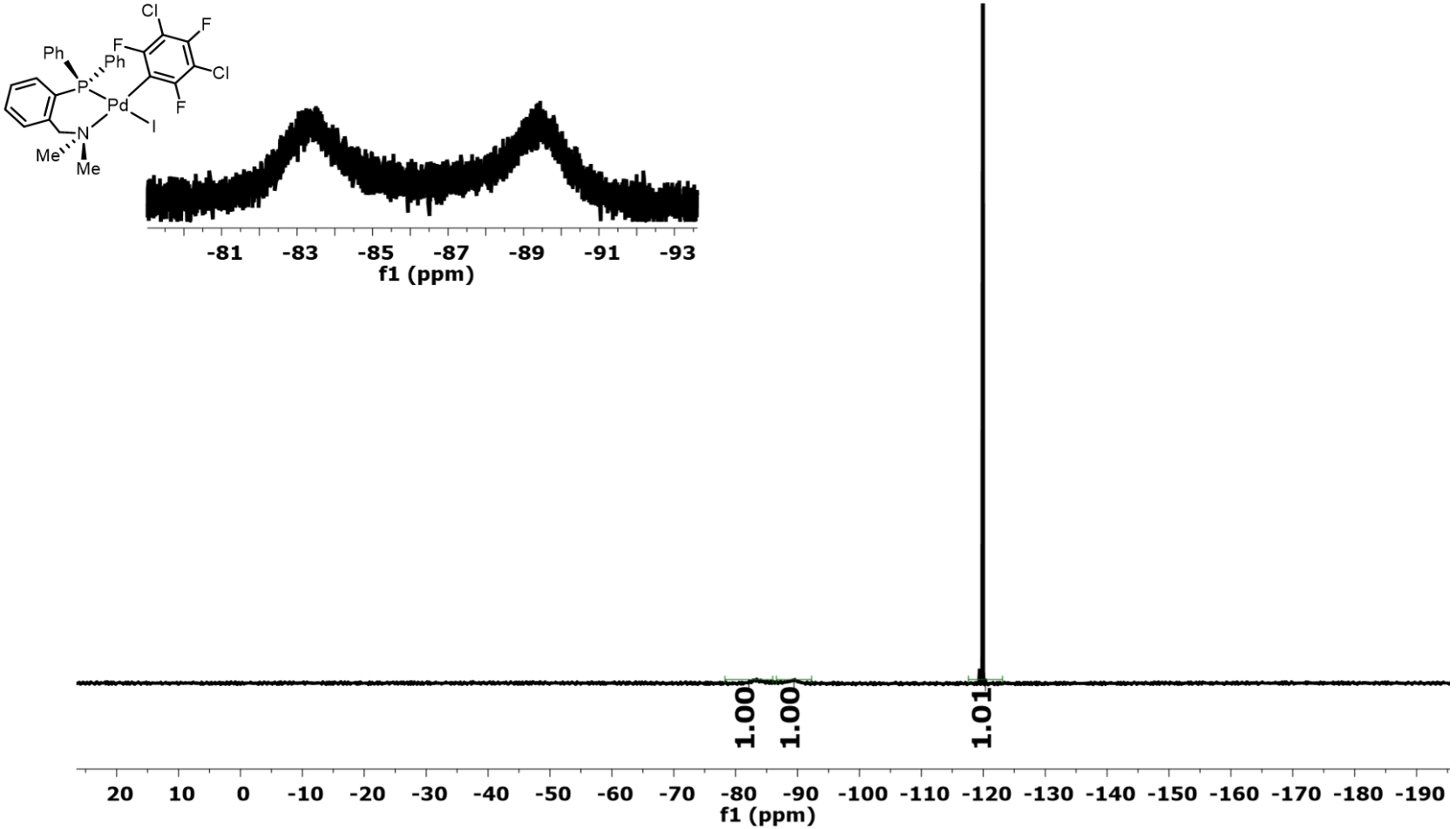

Figure ESI 27. ^{19}F NMR (470 MHz, $CDCl_3$, 298 K) of **3c**

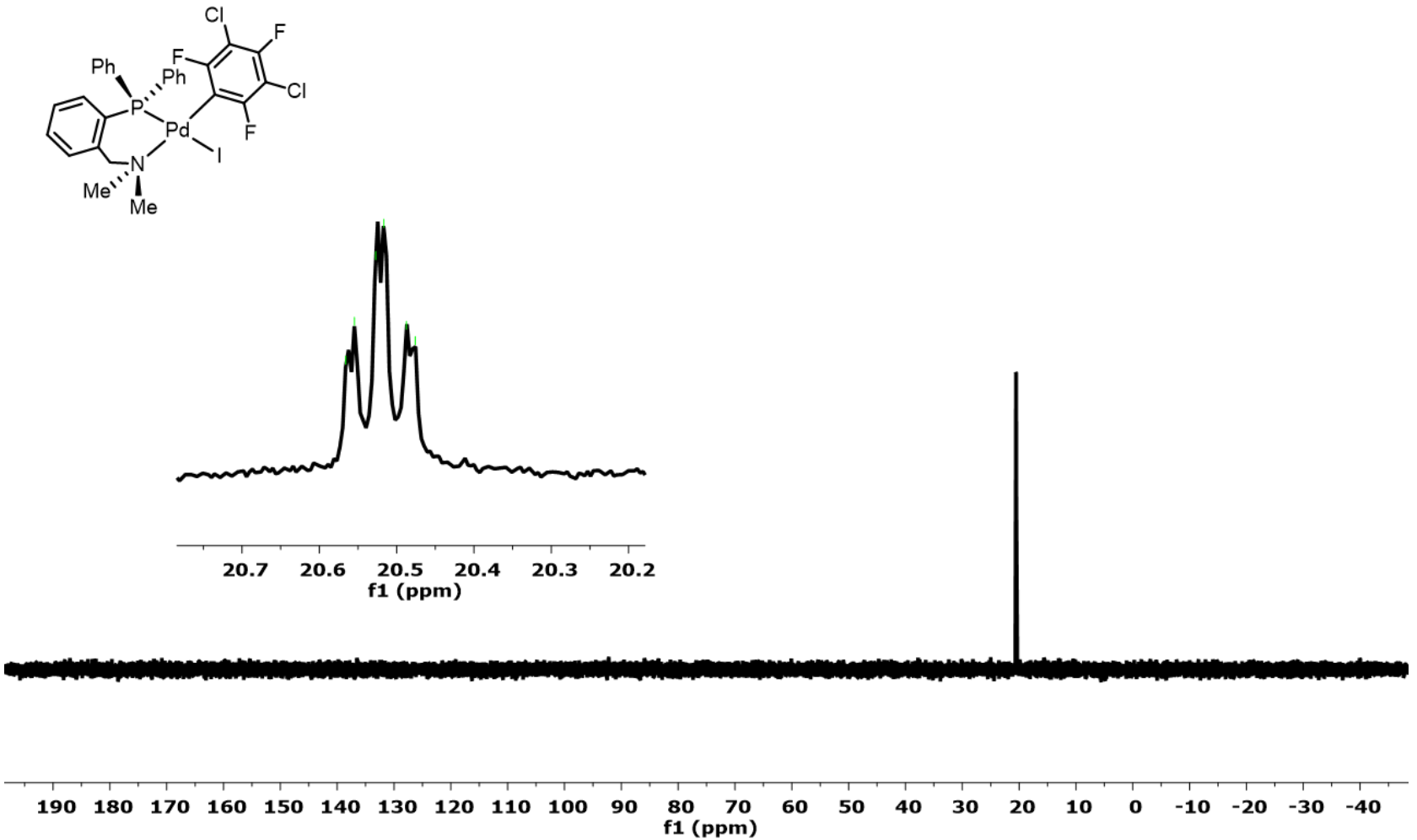

Figure ESI 28. $^{31}P\{^{1}H\}$ NMR (202 MHz, $CDCl_3$, 298 K) of **3c**

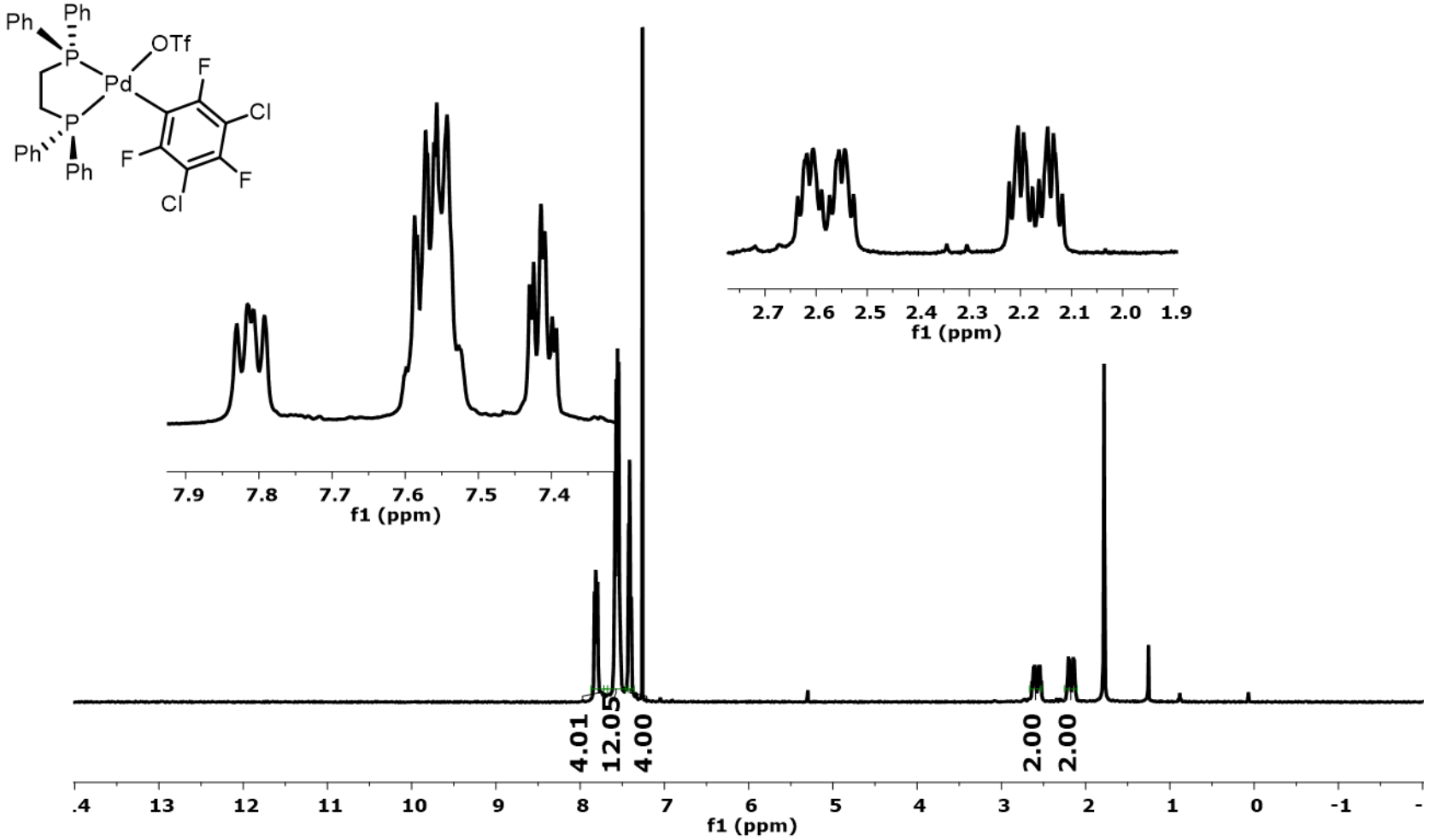

Figure ESI 29. ^{1}H NMR (500 MHz, $CDCl_3$, 298 K) of **4a**

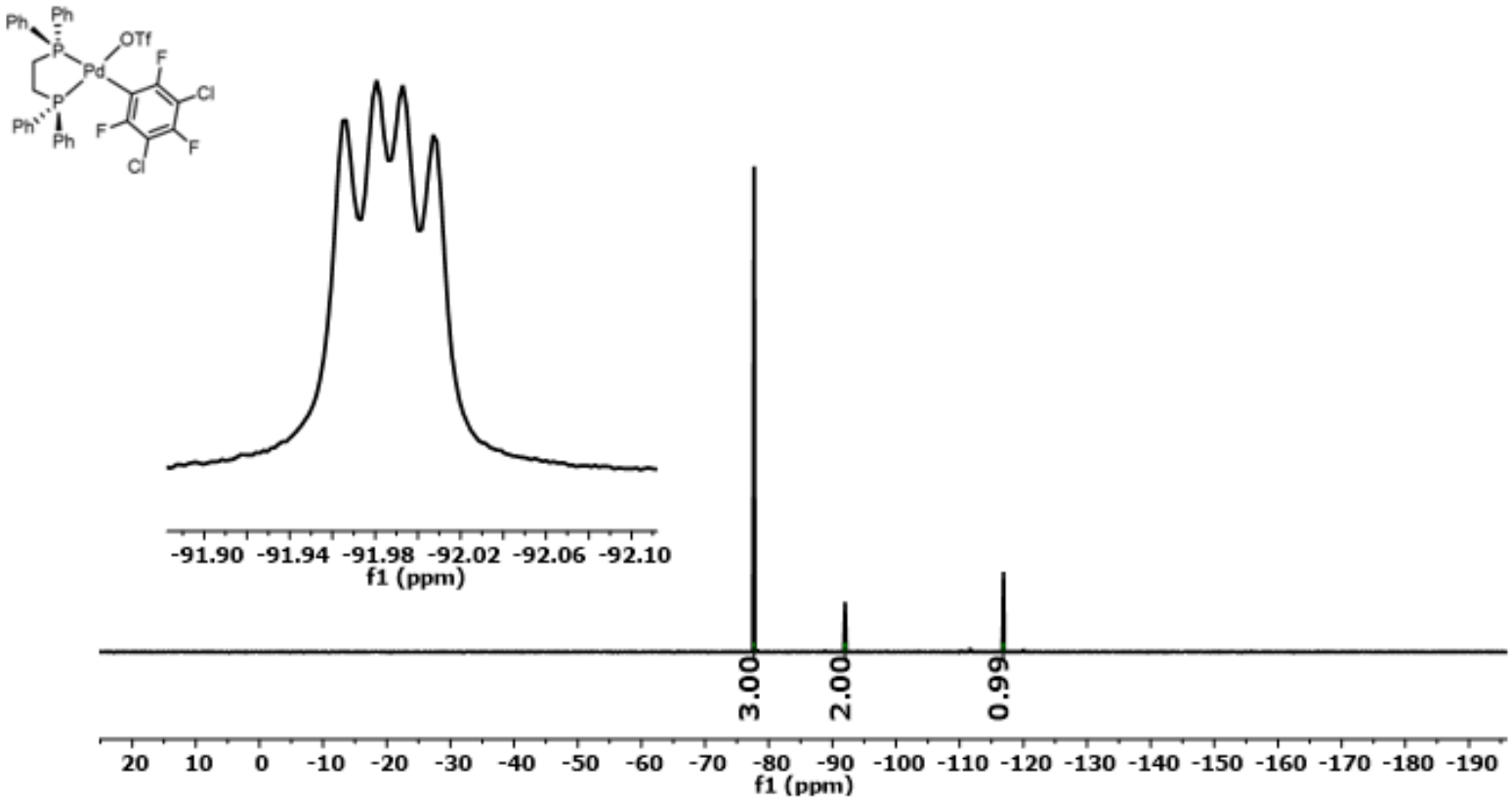

Figure ESI 30. ^{19}F NMR (470 MHz, $CDCl_3$, 298 K) of **4a**

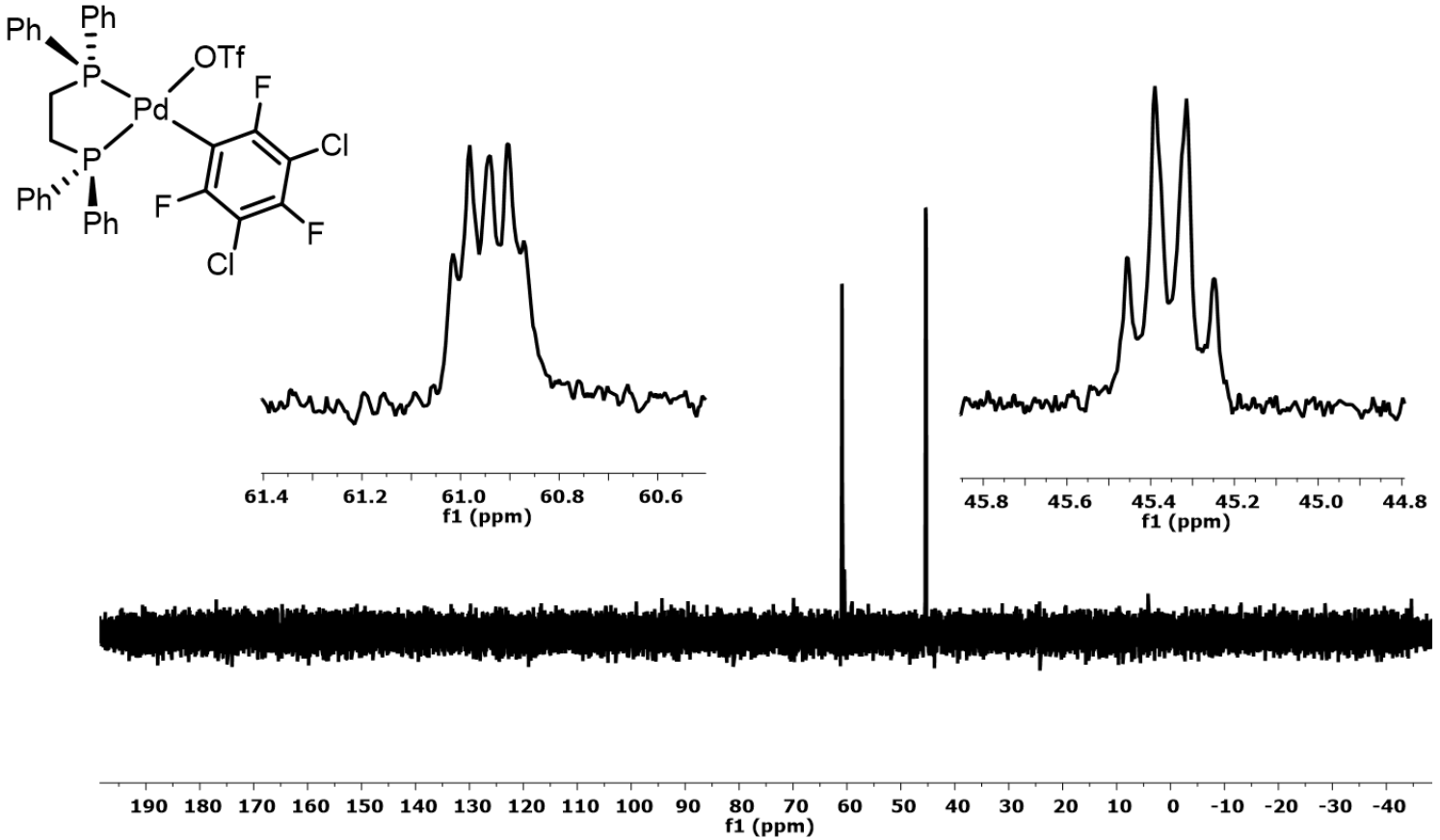

Figure ESI 31. $^{31}P\{^{1}H\}$ NMR (202 MHz, $CDCl_3$, 298 K) of **4a**

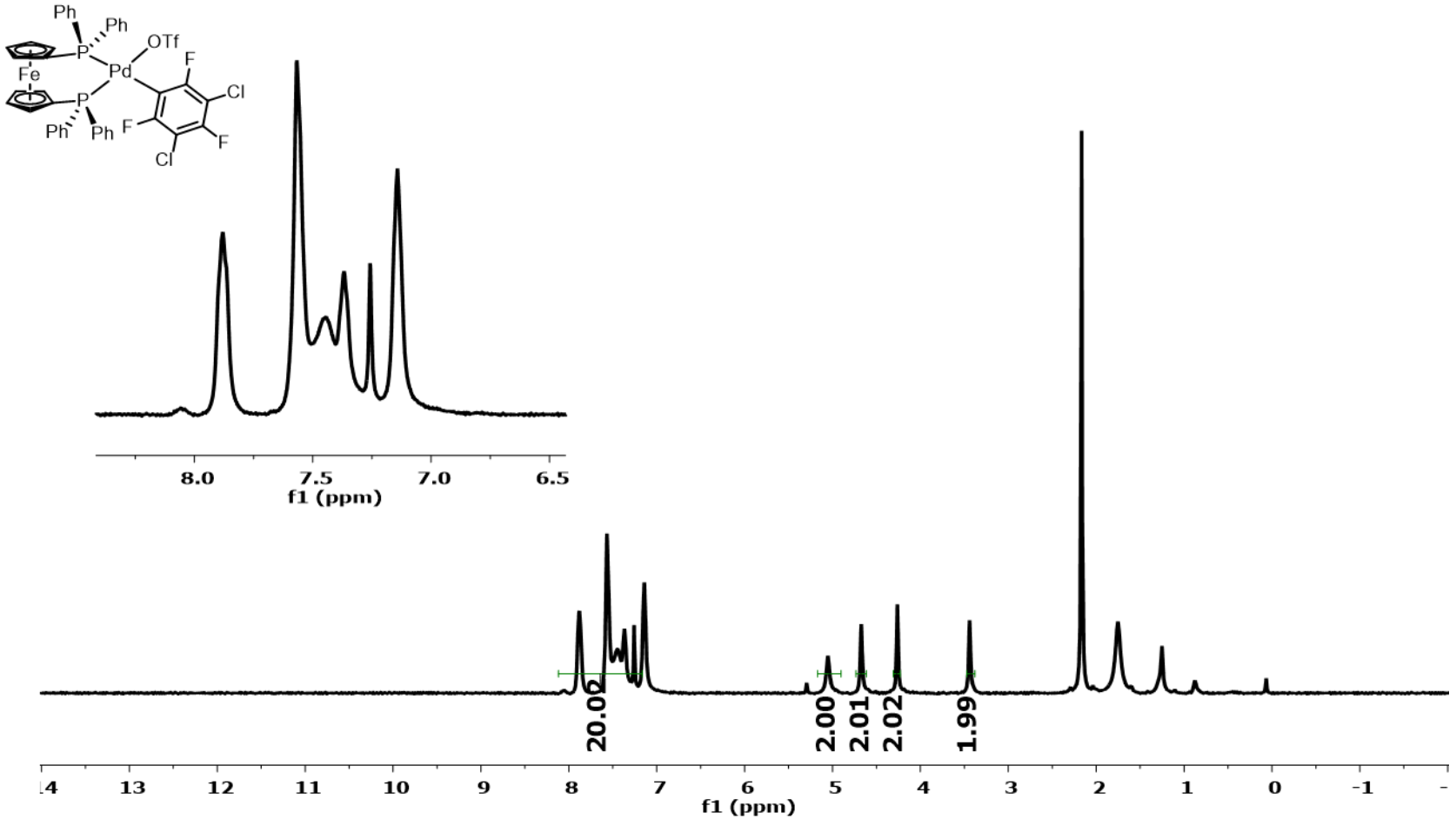

Figure ESI 32. ^{1}H NMR (400 MHz, $CDCl_3$, 298 K) of **4b**

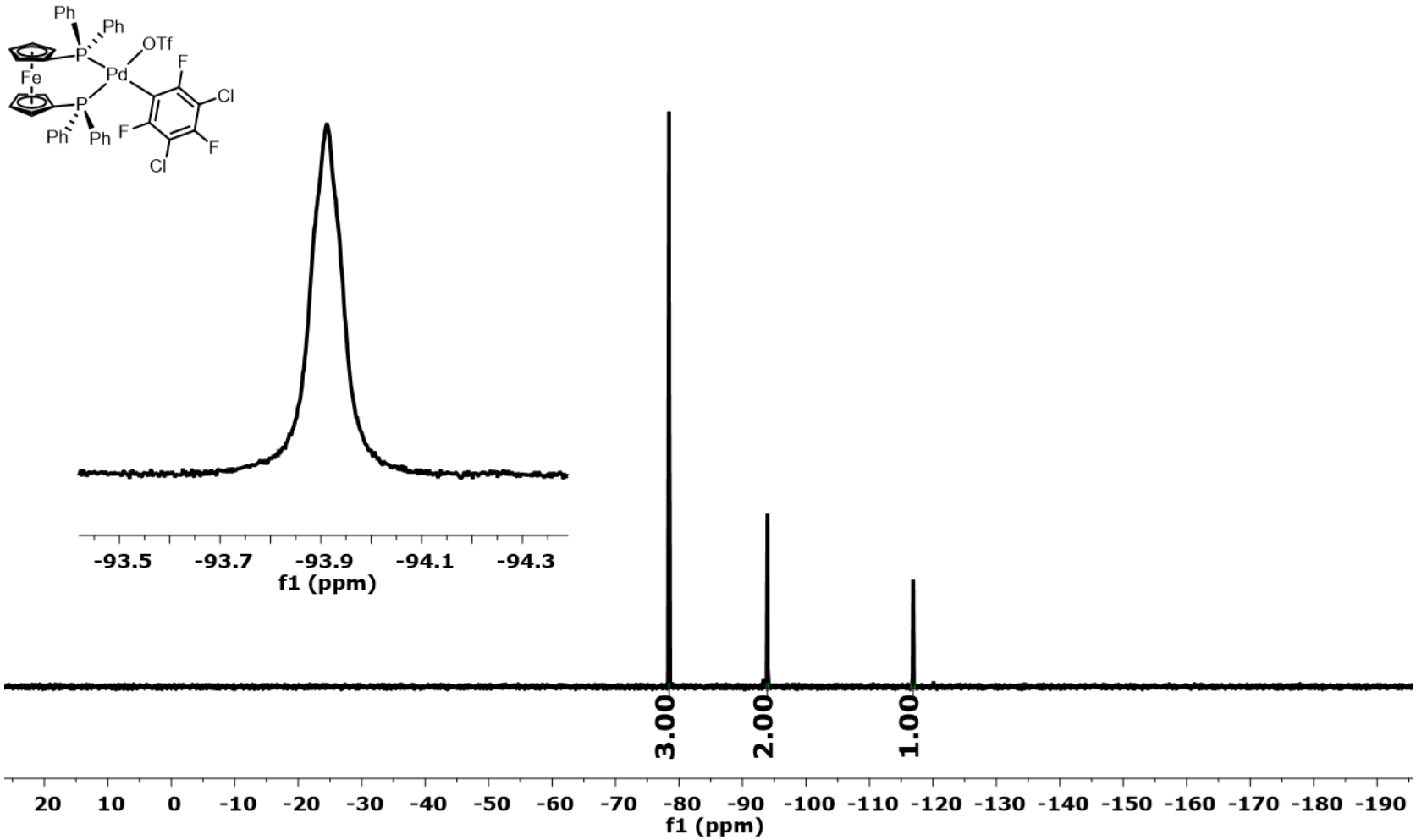

Figure ESI 33. ^{19}F NMR (376 MHz, $CDCl_3$, 298 K) of **4b**

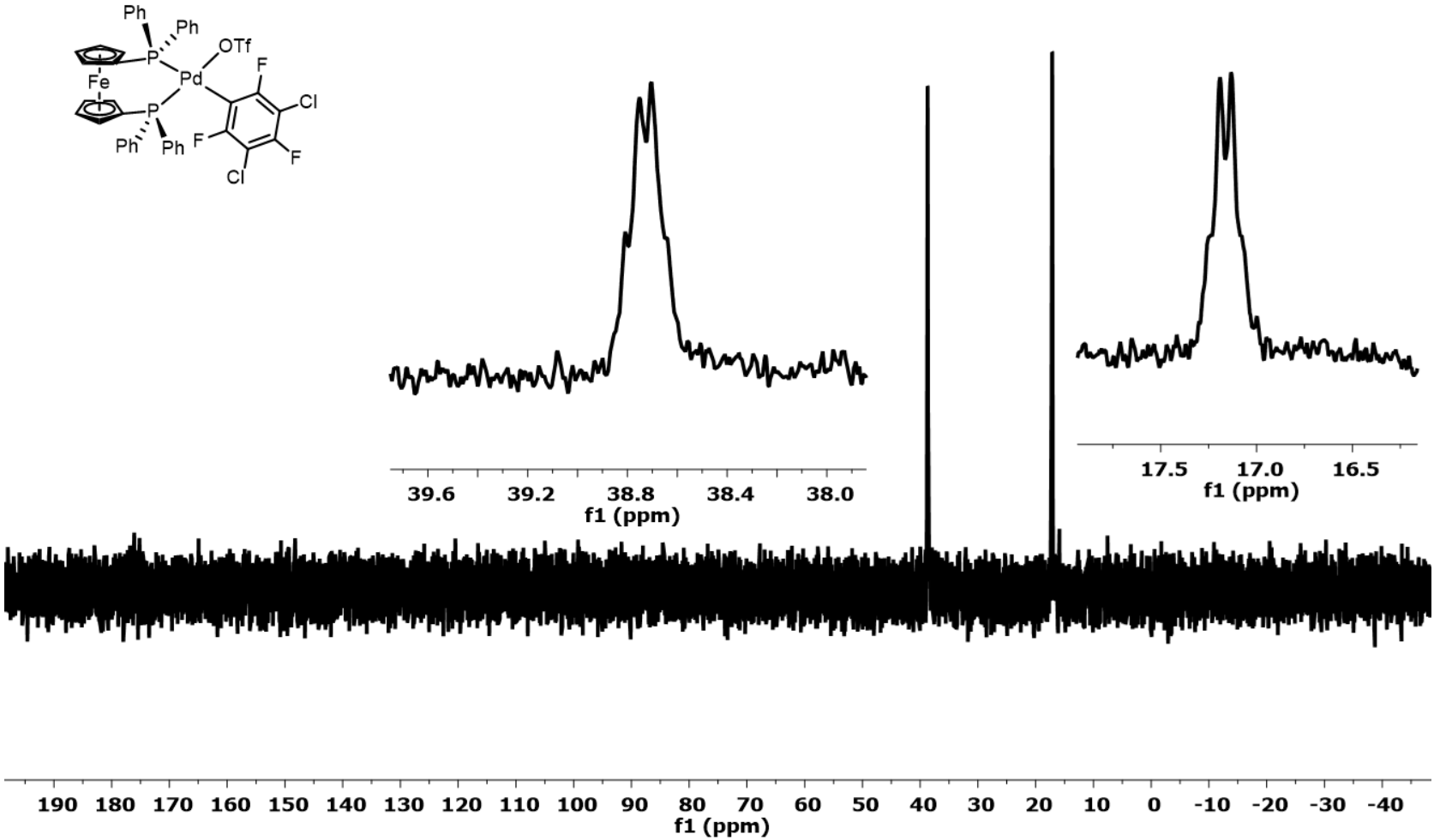

Figure ESI 34. $^{31}P\{^{1}H\}$ NMR (162 MHz, $CDCl_3$, 298 K) of **4b**

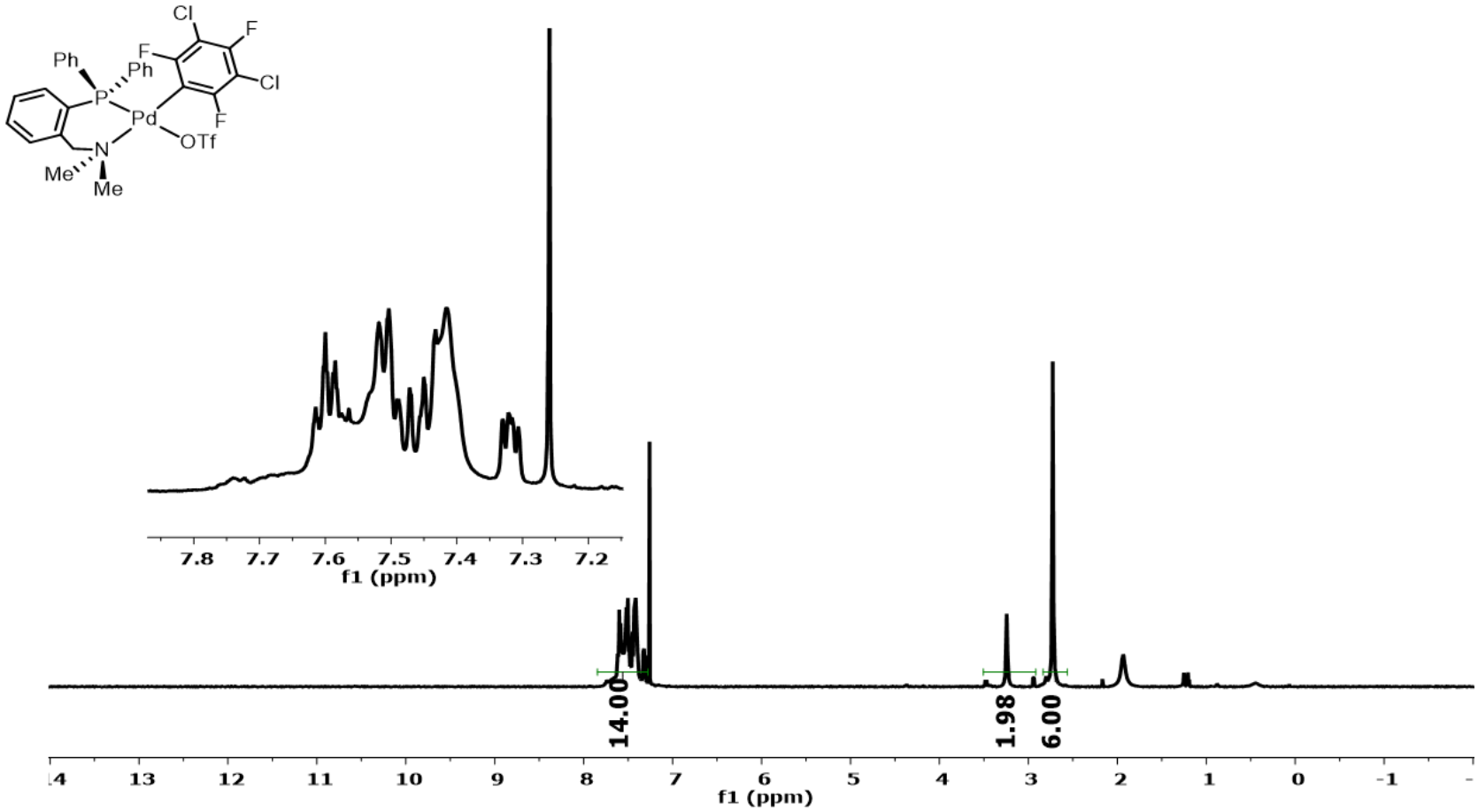

Figure ESI 35. ^{1}H NMR (400 MHz, $CDCl_3$, 298 K) of **4c**

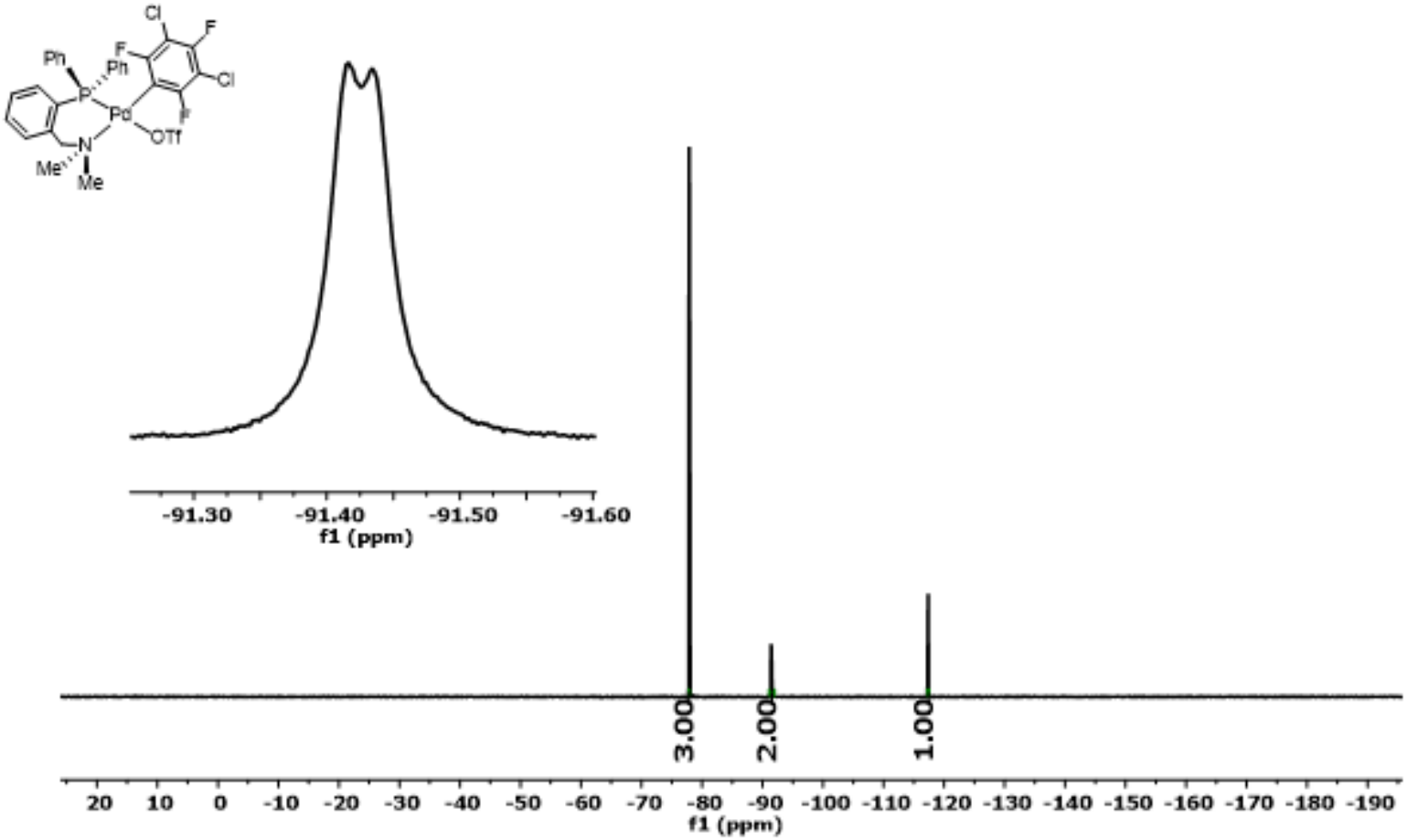

Figure ESI 36. ^{19}F NMR (376 MHz, $CDCl_3$, 298 K) of **4c**

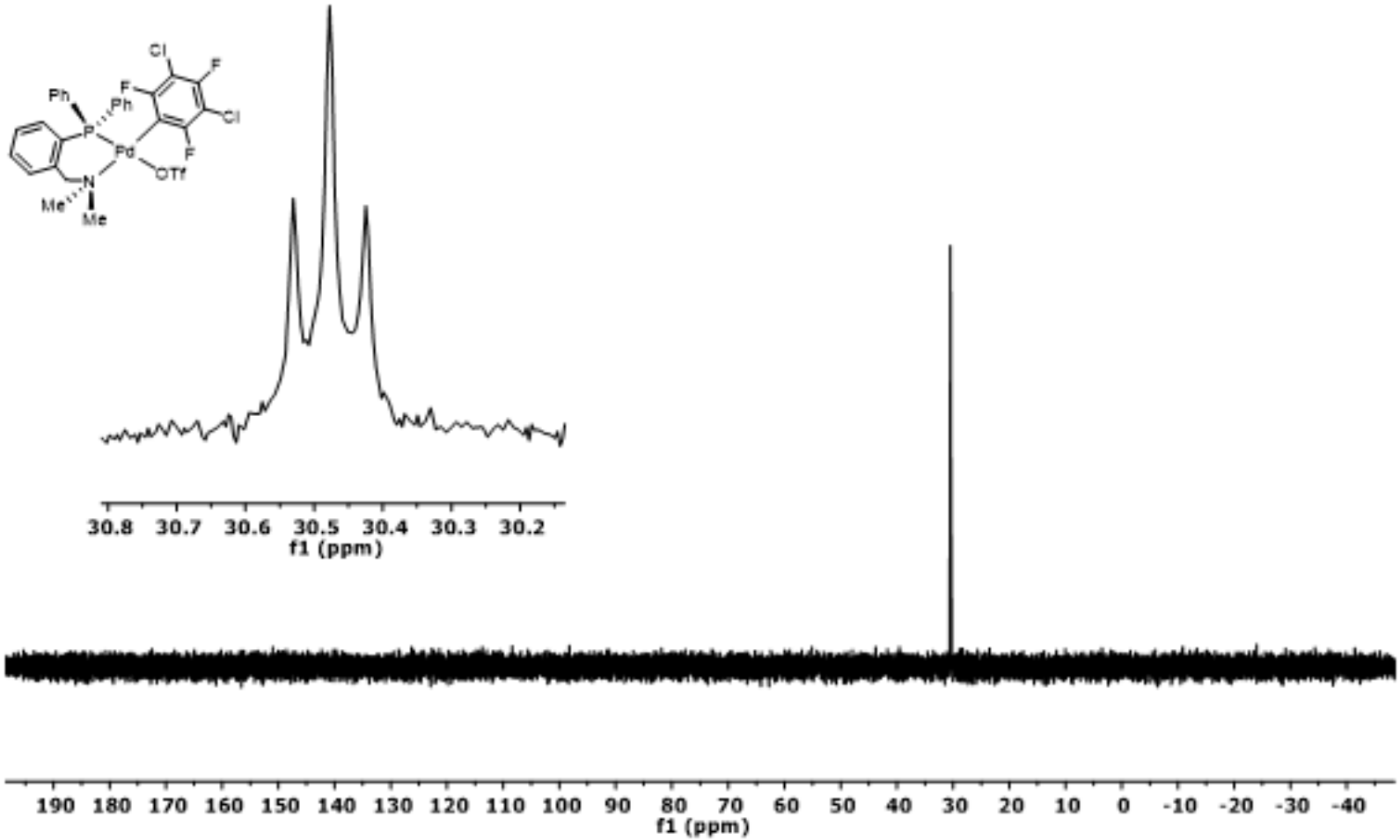

Figure ESI 37. $^{31}P\{^{1}H\}$ NMR (162 MHz, $CDCl_3$, 298 K) of **4c**

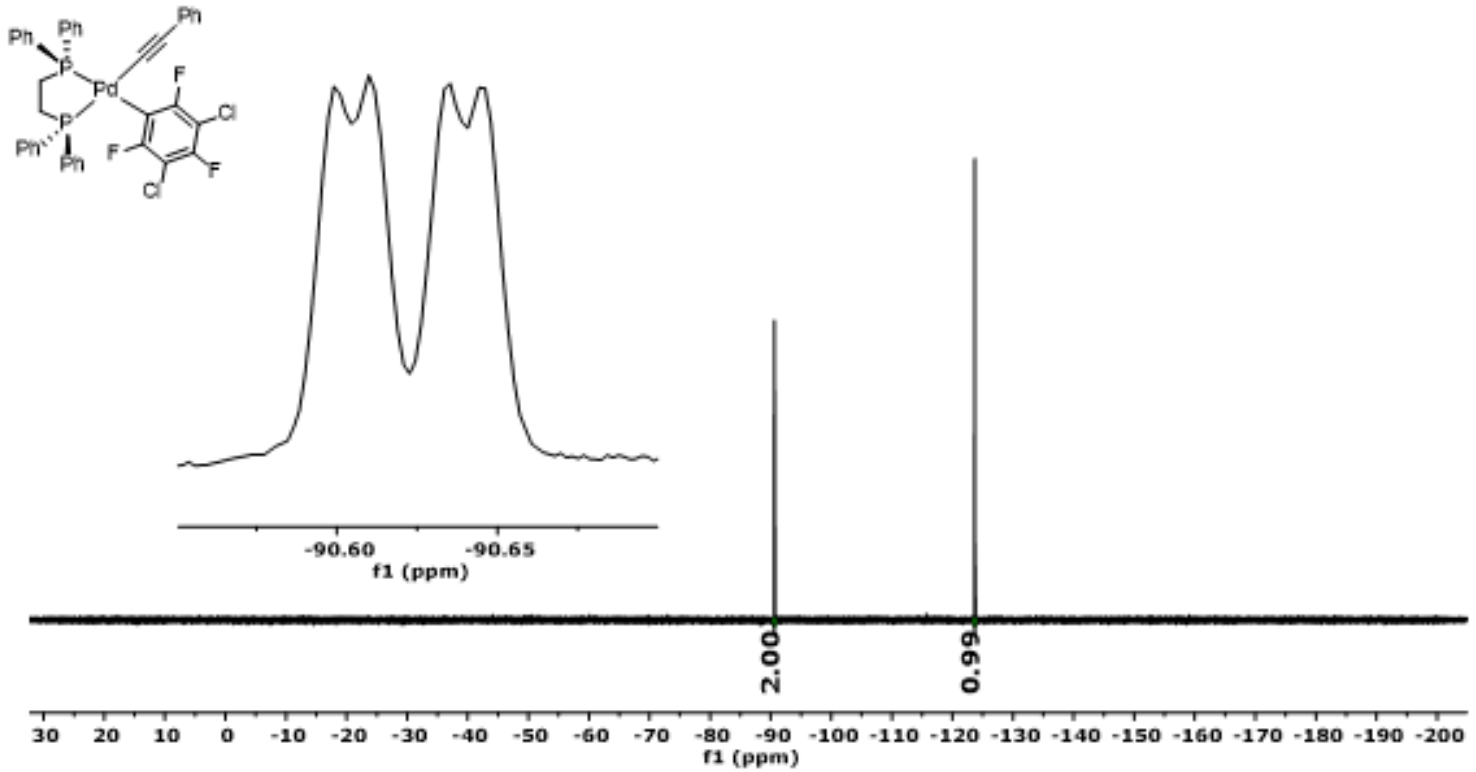

Figure ESI 38. ^{19}F NMR (376 MHz, THF/cap. acetone-d_6, 298 K) of **11a**

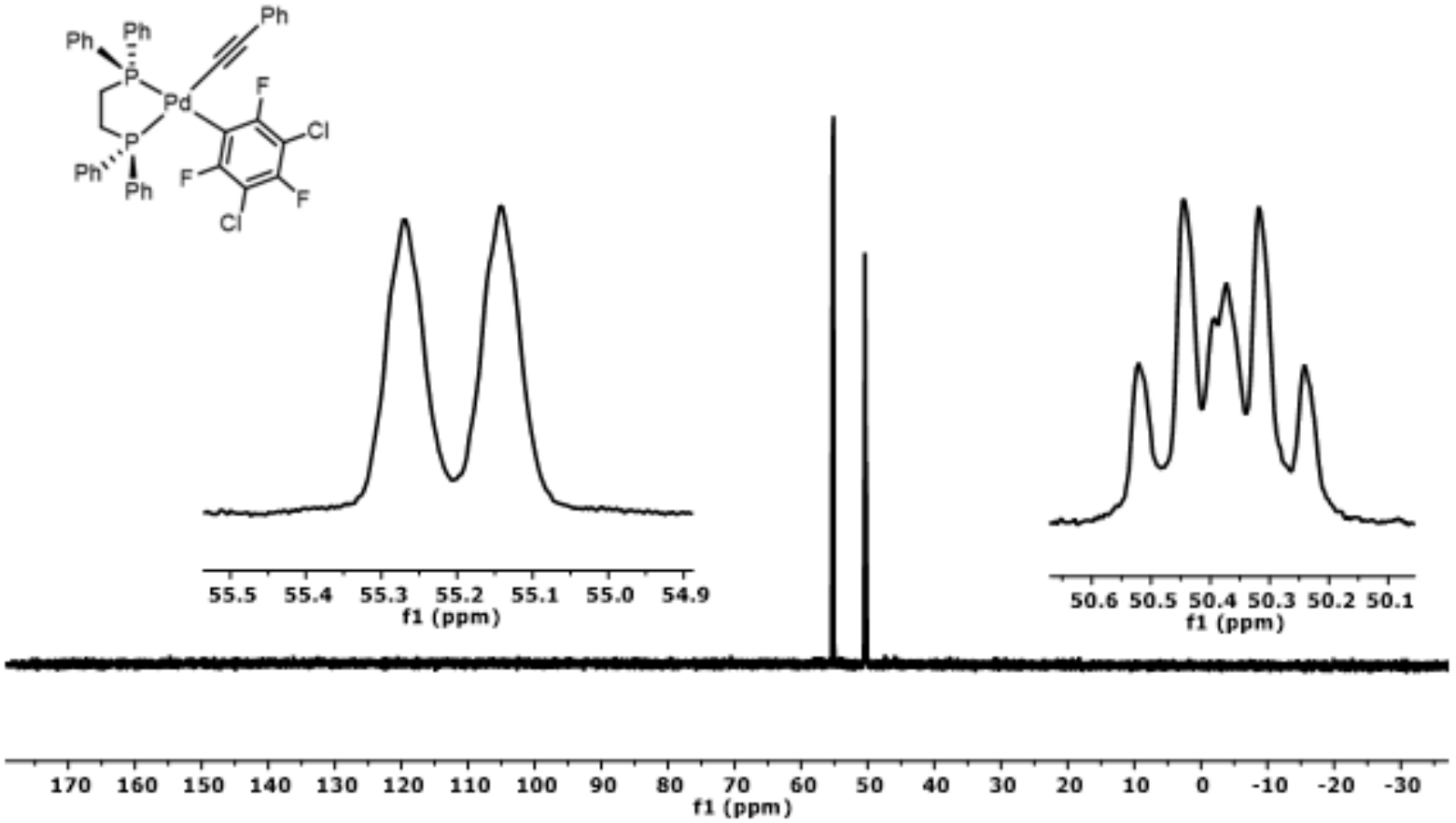

Figure ESI 39. $^{31}P\{^{1}H\}$ NMR (202 MHz, THF/cap. acetone-d_6,298 K) of **11**

12. References

1 D. B. G. Williams and M. Lawton, *J. Org. Chem.*, 2010, **75**, 8351–8354.

2 G. R. Fulmer, A. J. M. Miller, N. H. Sherden, H. E. Gottlieb, A. Nudelman, B. M. Stoltz, J. E. Bercaw and K. I. Goldberg, *Organometallics*, 2010**, 29**, 2176–2179.

3 P. Espinet, J. M. Martínez-Ilarduya, C. Pérez-Briso, A. L. Casado and M. A. Alonso, *J. Organomet. Chem.*, 1998, **551**, 9–20.

4 M. H. Pérez-Temprano, A. M. Gallego, J. A. Casares and P. Espinet, *Organometallics*, 2011, **30**, 611–617.

5 T. B. Rauchfuss, F. T. Patino and D. M. Roundhill, *Inorg. Chem.*, 1975, **14**, 652–656.

6 CrysAlisPro Software system, version 1.171.33.51, 2009, Oxford Diffraction Ltd, Oxford, UK.

7 O. V. Dolomanov, L. J. Bourhis, R. J. Gildea, J. A. K. Howard and H. Puschmann, *J. Appl. Cryst.*, 2009, **42**, 339–341.

8 G. M. Sheldrick, *Acta Cryst.*, 2015, **A71**, 3–8.

9 G. M. Sheldrick, *Acta Cryst.*, 2015, **C71**, 3–8.

10 C. Ammann, P. Meier and A. E. Merbach, *J. Magn. Reson.*, 1982, **46**, 319–321.

11 To calculate Keq for the neutral ⇌ ionic equilibria, the ionic species have been considered as ionic pairs in THF solution (A. Jutand and A. Mosleh, *Organometallics*, 1995, **14**, 1810–1817).

12 S. Hoops, S. Sahle, R. Gauges, C. Lee, J. Pahle, N. Simus, M. Singhal, L. Xu, P. Mendes and U. Kummer, *Bioinformatics*, 2006, **22**, 3067–3074.

13 J.-D. Chai and M. Head-Gordon, *Phys. Chem. Chem. Phys.*, 2008, **10**, 6615–6620.

14 Gaussian 09, Revision **E.01**, M. J. Frisch, G. W. Trucks, H. B. Schlegel, G. E. Scuseria, M. A. Robb, J. R. Cheeseman, G. Scalmani, V. Barone, G. A. Petersson, H. Nakatsuji, X. Li, M. Caricato, A. V. Marenich, J. Bloino, B. G. Janesko, R. Gomperts, B. Mennucci, H. P. Hratchian, J. V. Ortiz, A. F. Izmaylov, J. L. Sonnenberg, D. Williams-Young, F. Ding, F. Lipparini, F. Egidi, J. Goings, B. Peng, A. Petrone, T. Henderson, D. Ranasinghe, V. G. Zakrzewski, J. Gao, N. Rega, G. Zheng, W. Liang, M. Hada, M. Ehara, K. Toyota, R. Fukuda, J. Hasegawa, M. Ishida, T. Nakajima, Y. Honda, O. Kitao, H. Nakai, T. Vreven, K. Throssell, J. A., Jr. Montgomery, J. E. Peralta, F. Ogliaro, M. J. Bearpark, J. J. Heyd, E. N. Brothers, K. N. Kudin, V. N. Staroverov, T. A. Keith, R. Kobayashi, J. Normand, K. Raghavachari, A. P. Rendell, J. C. Burant, S. S. Iyengar, J. Tomasi, M. Cossi, J. M. Millam, M. Klene, C. Adamo, R. Cammi, J. W. Ochterski, R. L. Martin, K. Morokuma, O. Farkas, J. B. Foresman, D. J. Fox, Gaussian, Inc., Wallingford CT, 2009.

15 J. delPozo, D. Carrasco, M. H. Pérez-Temprano, M. García-Melchor, R. Álvarez, J. A. Casares and P. Espinet, *Angew. Chem., Int. Ed.*, 2013, **52**, 2189–2193.

16 (a) P. J. Hay and W. R. Wadt, *J. Chem. Phys.*, 1985, **82**, 270–283. (b) P. J. Hay and W. R. Wadt, *J. Chem. Phys.*, 1985, **82**, 299–310.

17 A. W. Ehlers, M. Böhme, S. Dapprich, A. Gobbi, A Höllwarth, V. Jonas, K. F. Köhler, R. Stegmann, A. Veldkamp and G. Frenking, *Chem. Phys. Lett.*, 1993, **208**, 111–114.

18 A. V. Marenich, C. J. Cramer and D. G. Truhlar, *J. Phys. Chem. B*, 2009, **113**, 6378–6396.

19 NBO 6.0. E. D. Glendening, J, K. Badenhoop, A. E. Reed, J. E. Carpenter, J. A. Bohmann, C. M. Morales, C. R. Landis and F. Weinhold, (Theoretical Chemistry Institute, University of Wisconsin, Madison, WI, 2013); http://nbo6.chem.wisc.edu/